Quaternary Science Reviews 198 (2018) 15–36

Contents lists available at ScienceDirect

Quaternary Science Reviews

journal homepage: www.elsevier.com/locate/quascirev

A continuous record of vegetation, fire-regime and climatic changes in northwestern Patagonia spanning the last 25,000 years

Patricio I. Moreno [a, *], Javiera Videla [a], Blas Valero-Garcés [b], Brent V. Alloway [c], Linda E. Heusser [d]

[a] Instituto de Ecología y Biodiversidad, Departamento de Ciencias Ecológicas, Universidad de Chile, Santiago, Chile
[b] Pyrenean Institute of Ecology, Spanish Scientific Research Council, Zaragoza, Spain
[c] School of Environment, The University of Auckland, Private Bag 92019, Auckland, New Zealand
[d] Lamont-Doherty Earth Observatory, Columbia University, New York, United States

ARTICLE INFO

Article history:
Received 25 May 2018
Received in revised form
11 August 2018
Accepted 13 August 2018
Available online 5 September 2018

Keywords:
Vegetation history
Fire disturbance
Northwestern patagonia
Southern westerly winds
Last glacial termination
Last glacial maximum
Holocene

ABSTRACT

We present a high-resolution precisely dated terrestrial paleovegetation/paleoclimate record from Lago Pichilaguna, northwestern Patagonia (40°–44°S), which spans continuously from the Last Glacial Maximum (LGM) to the present. We find abundant and continuous presence of arboreal pollen (chiefly *Nothofagus*) during the LGM, accompanied by other trees, shrubs, and alpine herbs. These results suggest Subantarctic parkland and/or scattered woodlands under a cold and hyperhumid climate during the LGM (~25,000–17,800 cal. yr BP) with expansion of *Nothofagus* under relatively warm interstadial conditions between 25,000 and 19,200 cal. yr BP. This was followed by cooling and a precipitation increase between 19,200 and 17,800 cal. yr BP, which was contemporaneous with the youngest LGM advance of Andean glaciers in the region and maximum influence of the Southern Westerly Wind (SWW). The Last Glacial Termination (T1) started at 17,800 cal. yr BP and featured the spread of thermophilous trees and ferns characteristic of North Patagonian rainforests, along with lake level lowering. These results suggest a warm pulse and southward shift of the SWW, concurrent with a rapid collapse of Andean glacier lobes. Subsequent changes led to the establishment of closed-canopy rainforests under peak interstadial warmth between ~16,000 and 15,000 cal. yr BP. We detect a shift to cold/wet conditions during the Antarctic Cold Reversal (14,800–12,700 cal. yr BP) and a precipitation decline during Younger Dryas time, followed by maximum temperature, relatively lower lake level and minimum SWW influence between 11,300 and 7700 cal. yr BP. Precipitation then rose punctuated by centennial-scale variations since 6200 cal. yr BP. Chilean-European deforestation and spread of invasive exotic species started at ~350 cal. yr BP aided by fire. We conclude that temperate rainforests have persisted with little interruption since T1, with major changes in floristic composition driven by climate change and fires. Rainforest composition and heterogeneity declined in response to Chilean/European disturbance during the 1600s and intensified since the 1800s. These events constitute the fastest/largest-magnitude vegetation changes of the last ~25,000 years.

© 2018 Elsevier Ltd. All rights reserved.

1. Introduction

A growing body of empirical (Denton et al., 2010) and modelling studies (Toggweiler, 2009; Toggweiler et al., 2006) have stressed the central role of the Southern Westerly Winds (SWW) as a critical paleoclimate link in the Southern Hemisphere. The SWW are fundamental in driving the Antarctic Circum-Polar Current, global deep-water circulation, upwelling of CO_2-enriched deep waters in the Southern Ocean (SO) and, consequently, atmospheric CO_2 concentrations. Despite their importance in modern and past climate dynamics, large uncertainties linger in the literature regarding their evolution and underlying mechanisms during and since the Last Glacial Maximum (LGM). In modern climate, the SWW are affected by tropical and extra-tropical modes of variability which modulate their strength, breadth and latitudinal position and, therefore, the delivery of moisture to all southern mid-latitude landmasses affecting natural environments and economic activities.

* Corresponding author.

https://doi.org/10.1016/j.quascirev.2018.08.013
0277-3791/© 2018 Elsevier Ltd. All rights reserved.

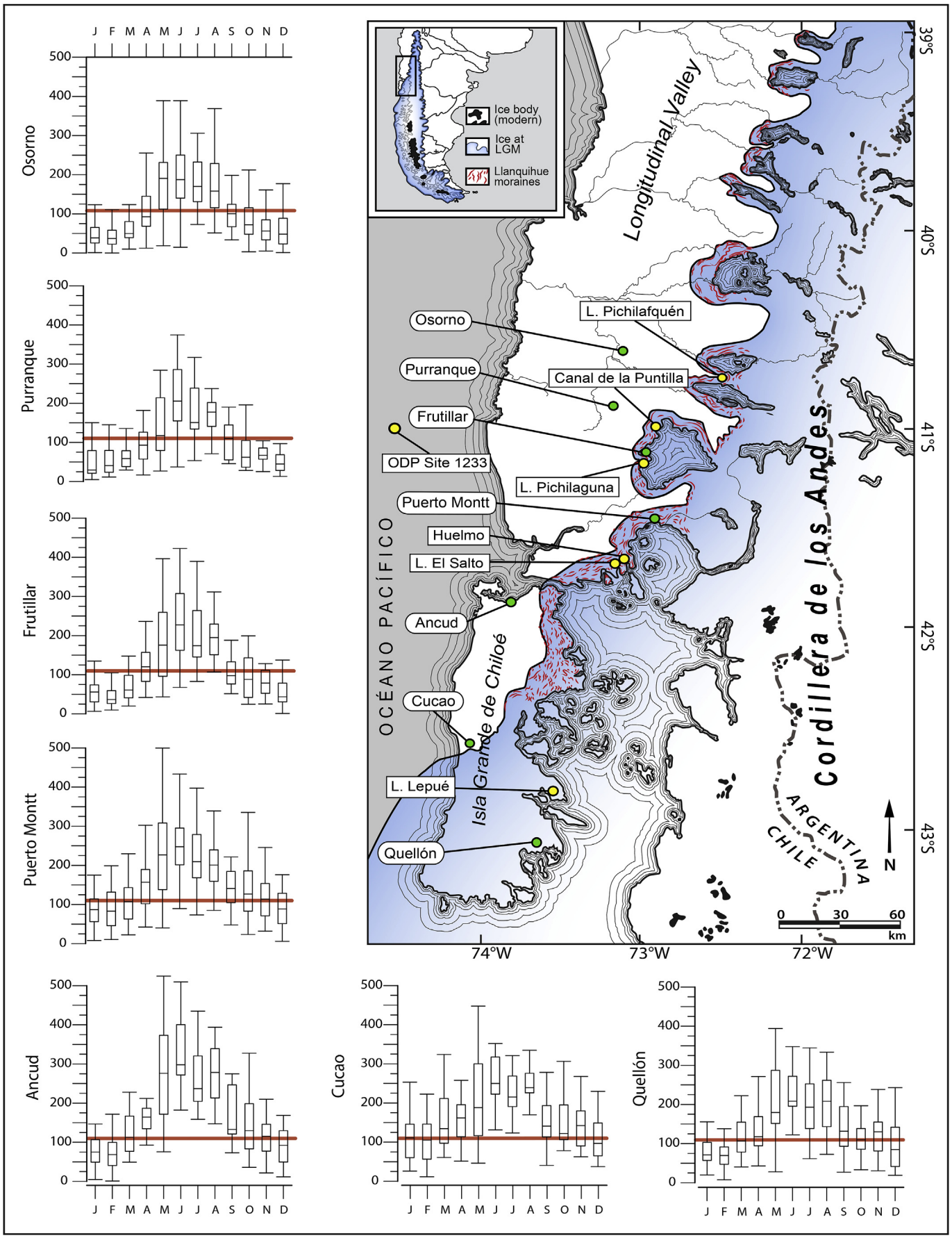
J F M A M J J A S O N D
Osorno
Purranque
Frutillar
Puerto Montt
Ancud
Cucao
Quellón
0
100
200
300
400
500
Ice body (modern)
Ice at LGM
Llanquihue moraines
Longitudinal Valley
Cordillera de los Andes
OCÉANO PACÍFICO
Isla Grande de Chiloé
Osorno
Purranque
Frutillar
ODP Site 1233
Puerto Montt
Huelmo
L. El Salto
Ancud
Cucao
L. Lepué
Quellón
L. Pichilafquén
Canal de la Puntilla
L. Pichilaguna
ARGENTINA
CHILE
N
0 30 60
km
39°S
40°S
41°S
42°S
43°S
74°W
73°W
72°W

The Pacific sector of northwestern Patagonia, in southern South America (40°–44°S), stands as key region for monitoring climate evolution in the middle latitudes of the Southern Hemisphere, including the behaviour of the SWW and their effects on vegetation, hydrology and fire occurrence. Piedmont glacier lobes originating from the Patagonian Ice Sheet descended westward from the Andes and covered the lowlands of the Chilean Lake District during the last glaciation, inducing shifts in the distribution and composition of terrestrial ecosystems which occupied ice-free sectors west and north of the ice margins (Heusser et al., 1999; Moreno et al., 1999). Past changes in moisture- and temperature-sensitive plant taxa recorded in paleovegetation records from this region suggest cold ($\Delta T = -6.5$ °C) and hyper-humid ($\Delta Pp = +2000$ mm/year) conditions (Heusser et al., 1999; Moreno et al., 2015) contemporaneous with the youngest advance of Andean ice lobes (between 19,300 and 17,800 cal. yr BP) during the LGM. The vegetation consisted of cold-resistant southern beech (*Nothofagus dombeyi* type), conifers (*Fitzroya cupressoides, Pilgerodendron uviferum, Podocarpus nubigena*) and Poaceae, attesting to a Subantarctic parkland (Heusser, 2003) or scattered woodland under cold and humid conditions. Pollen and charcoal data also suggest peak warmth and decline in precipitation, along with intense fire activity during the early Holocene (between 11,000 and 7800 cal. yr BP) (Moreno et al., 2015; Whitlock et al., 2007). These climatic states represent the end members for the total range of temperature and precipitation change during the most recent glacial-interglacial cycle, separated by a mere ~7000-year long interval during T1 within which prominent changes in paleoclimate took place at millennial timescales. A major transition at ~7600 cal. yr BP gave way to cooler/wetter conditions (Moreno, 2004; Moreno et al., 2018) for the remainder of the Holocene, and subsequent onset of centennial-scale changes in hydroclimate since ~5500 cal. yr BP (Moreno and Videla, 2016; Moreno et al., 2018). Varying degrees of coherence with records from other southern mid-latitude landmasses through time (Fletcher and Moreno, 2012) led to the interpretation of changes in the zonal symmetry of SWW through the Holocene, with a strongly symmetrical behaviour between 12,000 and 6000 cal. yr BP, and asymmetry over the last ~5500 years. To date, however, no single terrestrial record from Patagonia has the temporal resolution, chronologic precision, continuity and sensitivity to document paleovegetation and paleoclimate change along a temporal continuum from the LGM to the present.

In this study we examine past sedimentary, vegetation, fire-regime and climatic changes from sediment cores we collected from Lago Pichilaguna (41°15′55.63″S, 73° 3′31.71″W, 1.3 km^2, 110 m.a.s.l.), a small closed-basin lake located in the lowlands of the Chilean Lake District (Figs. 1 and 2). These data allow assessment of key questions: Did SWW influence increase (relative to the present) during the LGM? What was the timing and structure of paleoclimate signals during T1? How did SWW variability evolve through Holocene? Was there a shift from multi-millennial to centennial-scale variability during the mid-Holocene? We are also interested in examining the response of terrestrial ecosystems to disturbance regimes under different climatic scenarios, assessing the role of Chilean-European disturbance on vegetation structure and composition, and tracking the spread of exotic invasive species.

1.1. Study area

The Chilean Lake District, in northwestern Patagonia (40°–43°45′S), features the high-elevation, glaciated and volcanically active Andes Cordillera to the east, a lower-elevation, unglaciated and volcanically inactive Coastal Range to the west, and the Longitudinal Valley, a north-south trending tectonic depression bounded by these cordilleras (Fig. 1). The Longitudinal Valley contains glacial and volcanic deposits of Quaternary age and multiple large lakes of glacial origin that extend westward from the Andean massif. The Coastal Range diminishes in elevation and eventually disappears along a ~100 km gap between 40°20′S and 42°06′S and reappears in Isla Grande de Chiloé, the largest and westernmost island of the Chilotan archipelago. The Longitudinal Valley disappears south of Puerto Montt and gives way to the Seno Reloncaví seaway and the interior Chilotan Sea, in turn, connected to Golfo Corcovado and the Pacific Ocean along its southern limit (Fig. 1). Lago Pichilaguna is a relatively small (1.3 km^2) and shallow (<20 m water depth) lake, located in a closed-basin drainage watershed atop a moraine complex deposited by the Lago Llanquihue ice lobe on the Longitudinal Valley of the Chilean Lake District during the last glaciation (Denton et al., 1999b).

The climate of western Patagonia is under the permanent influence of the SWW, which constitute the sole source of precipitation along the Pacific slopes of the Andes Cordillera. Local precipitation shows a strong positive correlation with zonal wind speeds along a broad sector of the southern mid-latitudes (Garreaud, 2007), implying that precipitation amount in this sector is a good diagnostic for (present and past) SWW behaviour at zonal scale. The present-day climate in the Chilean Lake District is temperate and wet, i.e. mean annual temperature and precipitation in the lowlands of the Longitudinal Valley are 10 °C and 10.5 °C (min: 6.4 °C and 5.4 °C, max: 14.9 °C and 16.6 °C) and 1725 and 1318 mm/year, in the Puerto Montt (41°43′S, 73°09′W, 85 masl) and Osorno (40°60′S, 73°06′W, 55 masl) meteorological stations respectively (Fig. 1). Precipitation occurs year-round with maximum values during the winter months and minimum values during the summer months (Fig. 1), affecting the occurrence of natural or human-induced fires. Instrumental records and reanalysis data have revealed a reduction in annual precipitation over the last 60 years, as a result of an intensification and poleward shift of the SWW, which has been widely attributed to the depletion of the ozone layer as well as the increase of atmospheric greenhouse gas emissions (Fogt et al., 2011; Thompson et al., 2011). Precipitation seasonality increases toward the north as shown by the monthly and annual precipitation in the region (Fig. 1). These measurements also indicate lengthening and deepening of the summer moisture deficit in the Longitudinal Valley, here defined arbitrarily as monthly precipitation values below 110 mm. Meteorological stations located near the coast typically exhibit modest moisture deficit values with up to three months with medians below the threshold during the summer months. Stations located in the Longitudinal Valley north of 41°20′S, on the other hand, show an extended deficit that lasts seven (stations Frutillar, Purranque) to eight months (station Osorno) (Fig. 1). This seasonality results from a combination of the increasing influence of the Southeastern Pacific Anticyclone at subtropical latitudes (Garreaud et al., 2009) and the rainshadow effect of the Coastal Range over the lowlands of the Longitudinal Valley.

Fig. 1. Map of the study area showing the location of palynological sites discussed in the text (yellow dots): Lago Pichilaguna, Lago Pichilafquén, Canal de la Puntilla, Huelmo, Lago El Salto, Lago Lepué, and ODP site 1233. Also shown are the location and box-whisker plots of the monthly precipitation data from relevant meteorological stations (green dots in the map). The red line in the precipitation diagrams represents an arbitrary threshold of 110 mm/month to illustrate the magnitude and duration of summer moisture deficit through the annual cycle. Mapped moraines west of the major lakes and gulfs are shown as red lines, along with the reconstructed extent of Andean piedmont ice lobes during the last glacial maximum. (For interpretation of the references to color in this figure legend, the reader is referred to the Web version of this article.)

The mountainous and archipelagic physiography of northwestern Patagonia, along with latitudinal and altitudinal gradients in temperature and precipitation, induces a marked zonation of the vegetation at regional scale. Temperate broad-leaved rainforests were the dominant vegetation in northwestern Patagonia prior to European settlement. At least three centuries of agrarian and forestry activities have decimated the native vegetation (Jara and Moreno, 2012, 2014; Moreno and Videla, 2016), which today is confined to parts of the Coastal Range and the western Andean flanks and foothills. The distribution and composition of the forest communities along environmental gradients in these sectors can be used as modern analogues for interpreting palynological records and inferring past climate changes. In the following paragraphs we provide a brief description of the major plant communities in the study area, detailed descriptions of the native vegetation in northwestern Patagonia can be found on Villagrán (1985), Heusser (1966), Heusser et al. (1999), Oberdorfer (1960) and Schmithüsen (1956).

- Lowland deciduous southern beech forest: present in the Longitudinal Valley of the Chilean Lake District with its southern limit at latitude ~41°S. Intense agriculture and forestry has decimated much of this forest community which features dominance of the deciduous *Nothofagus obliqua*, along with *Laurelia sempervirens, Persea lingue* and the conifer *Podocarpus saligna.* Forest gaps or edges commonly present the shrub *Aristotelia chilensis* and the bamboo *Chusquea quila.*
- Valdivian rainforest: this community is distributed south of the deciduous forest from the lowlands of the Longitudinal Valley upslope to ~400 m.a.s.l., and features the highest plant diversity in the region. The forest canopy is dominated by *Eucryphia cordifolia*, *Aextoxicon punctatum* and, to a lesser degree, by the evergreen beech *Nothofagus dombeyi* and its mistletoe *Misodendrum,* several species of the myrtle family (*Myrceugenia planipes*, *Amomyrtus luma*, *Luma apiculata*), the trees *Caldcluvia paniculata*, *Lomatia hirsuta* and *Gevuina avellana*, along with the vines *Hydrangea serratifolia*, *Cissus striata* and *Mitraria coccinea.* A diverse array of ferns such as *Polypodium feuillei*, *Lophosoria quadripinnata* and multiple species of *Hymenophyllum* occur on the forest floor, on standing and fallen trees. Dominant species in forest gaps are *E. cordifolia*, *A. chilensis,* and *Chusquea quila.*
- North Patagonian rainforest: this forest community occurs in the Andes between 400 and 900 m.a.s.l. and is dominated by the evergreen beech *Nothofagus dombeyi*, along with *Weinmannia trichosperma*, *Drimys winteri*, *Tepualia stipularis*, *Amomyrtus meli*, and *A. luma.* Above 600 masl *N. dombeyi* is accompanied by the cold-resistant conifers *Saxegothaea conspicua*, *Podocarpus nubigena*, *Fitzroya cupressoides* and *Pilgerodendron uviferum.*
- Deciduous Subantarctic forests: located in cooler and/or drier sectors with higher seasonality (400–1000 mm/year; 900–1180 m.a.s.l.). The dominant tree is *Nothofagus pumilio*, which intermingles with *N. betuloides* in western sites and the High Andean Desert in the alpine zone. *N. pumilio* forms monospecific stands and presents a species-poor understory (*Escallonia alpina, Berberis* spp., *Drimys andina*, *Maytenus disticha*). A study of the spatial and temporal variation in *N. pumilio* growth at treeline along its latitudinal range (from 35°40′S to 55°S) in the Chilean Andes (Lara et al., 2005) showed that temperature has a spatially larger control on tree growth than precipitation, and that this influence is particularly significant in the southern Andes (>40°S). These results suggest that low temperatures are the main limiting factor for the occurrence of woodlands and forests at high elevations in the Andes, considering that precipitation increases with elevation at any given latitude (Lara et al., 2005). The modern treeline in the Chilean Lake District is dominated by *N. pumilio* and lies between 1000 and 1200 m.a.s.l.
- High Andean Desert (alpine meadows): occurs in the windswept montane environments above the treeline (>1200 m.a.s.l.) under cold conditions, high precipitation regime and prolonged snow cover throughout the year. Vegetation cover in this unit is low, with scattered occurrence of herbs of the families Poaceae (*Poa, Festuca*), Asteraceae (*Nassauvia*, *Senecio*, *Perezia*), Rubiaceae (*Oreopulus*), Apiaceae (*Bolax*), Ericaceae (*Gaultheria, Empetrum*), along with *Gunnera magellanica* and *Valeriana*, and occasional patches of *Nothofagus antarctica.*
- Magellanic Moorland: this unit occurs in maritime sectors with high precipitation (3000–4000 mm/year and low seasonality) along the islands, fjords and channels, as well as the mountaintops of the cordilleras in the Chilean Lake District. Magellanic Moorland communities are dominated by cushion-forming plants such as *Donatia fascicularis, Astelia pumila* and *Tetroncium magallanicum.* Also present are the hygrophilous cold-resistant trees *Nothofagus betuloides* and the conifers *Pilgerodendron uviferum, Lepidothamnus fonkii* and *Podocarpus nubigena.*

2. Materials and methods

We obtained sediment cores from the deepest sector of Lago Pichilaguna (18 m water depth) (Figs. 1–3) during the years 2009 and 2014, using an Uwitec coring equipment and platform. Cores were logged using a Geotek Multi Sensor Core Logger (MSCL) at the Limnological Research Center (LRC), University of Minnesota, split and imaged with a DMT Core Scanner. We identified sedimentary facies following LRC procedures (Schnurrenberger et al., 2003) that include visual inspection, smear slides, sediment color, lithology and sedimentary structures. The core was sub-sampled for Total Organic Carbon (TOC), Total Inorganic Carbon (TIC) and Total Sulfur (TS) every 5 cm and analyzed with a LECO SC 144DR furnace at the Pyrenean Institute of Ecology (IPE-CSIC), Spain. X-ray fluorescence (XRF) data were obtained with an ITRAX core scanner from the Large Lake Observatory (Duluth, University of Minnesota) at 5 mm resolution (Mo and Cr tube at 30 kV and 20 mA measuring for 60 s). Results are expressed as element intensities in counts per second (cps) and ratios between diagnostic elements.

We processed continuous/contiguous sediment samples (1 cc) both for pollen and macroscopic fossil charcoal analyses. Pollen processing followed standard procedures that include 10% KOH, sieving with a 120 μm mesh, 46% HF and acetolysis (Faegri and Iversen, 1989). We counted 300 pollen grains produced by trees, shrubs and herbs for each palynological sample and calculated the percent abundance of each terrestrial taxon relative to this sum (terrestrial pollen). The percentage of aquatic plants was calculated in reference to the total pollen sum (terrestrial + aquatic pollen) and the percentage of ferns from the total pollen and spores sum. Zonation of the pollen record was aided by a stratigraphically constrained cluster analysis on all terrestrial pollen taxa having ≥2%, after recalculating sums and percentages. We then calculated the rates of change parameter based on the same data by smoothing 5 adjacent levels, square-root transformation and interpolating at 150 years intervals (Grimm and Jacobson, 1992).

We identified the palynomorphs based on a modern reference collection housed at the laboratory of Quaternary Paleoecology of Universidad de Chile, along with published descriptions and keys (Heusser, 1971; Villagrán, 1980). In most cases the identification was done at family or genus level, and in some cases to the species level (*Podocarpus nubigena, Drimys winteri, Gunnera magellanica, Lycopodium magellanicum*). The palynomorph *Nothofagus dombeyi* type includes the species *N. antarctica, N. pumilio, N. betuloides and N. dombeyi*, the morphotype *Fitzroya/Pilgerodendron* includes the

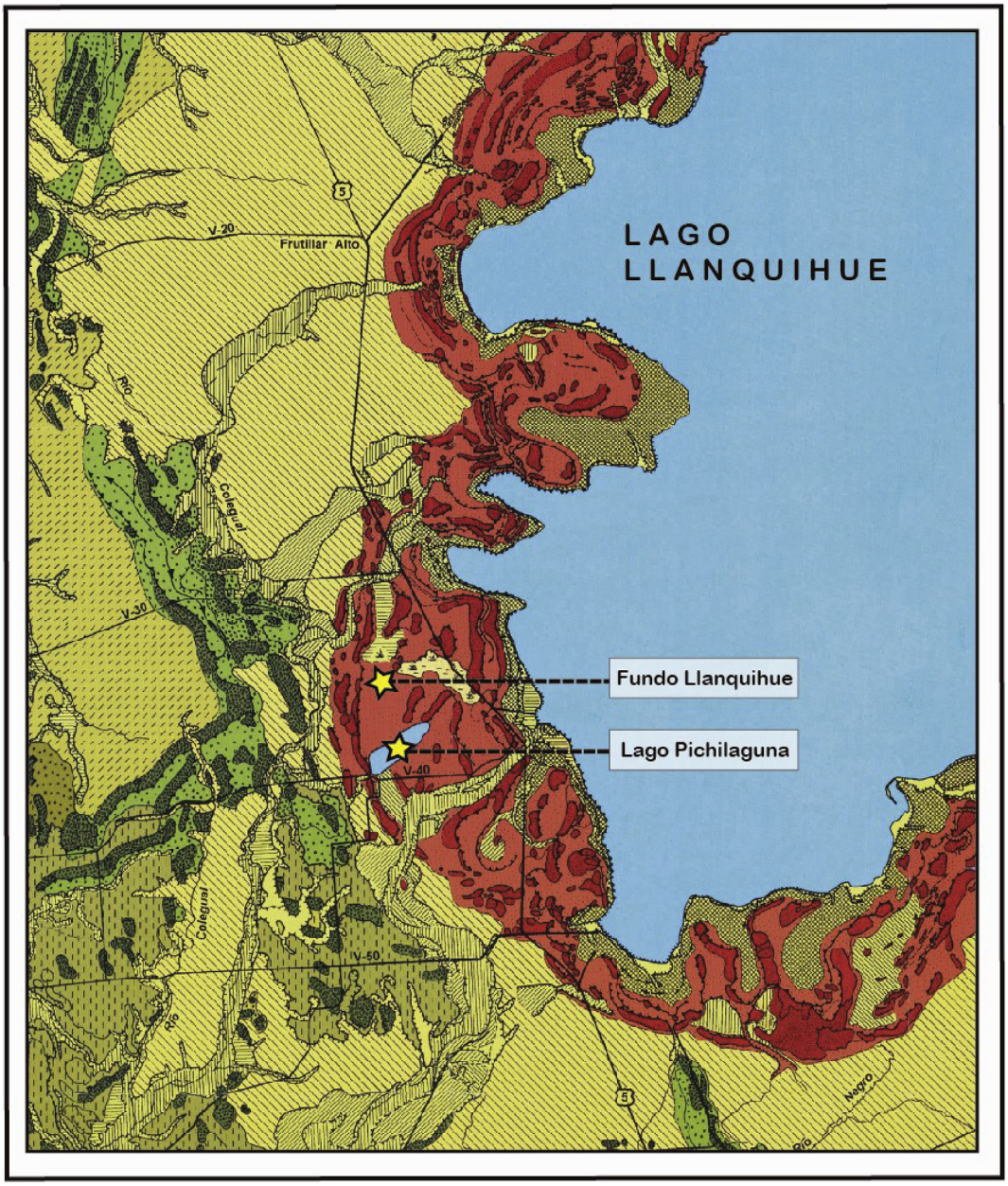

Fig. 2. Glacial geomorphologic map of the Lago Pichilaguna sector extracted from Andersen et al. (1999). The red and bright red sectors represent moraines deposited during the last glacial maximum (Llanquihue glaciation), the dark green and bright green areas represent pre-Llanquihue moraines. The yellow sectors with oblique stippled pattern represent outwash plains deposited distal to the Llanquihue-aged moraines, eventually dissected by meltwater channels originating from them. The largest of these is located ~7 km south of Lago Pichilaguna and is occupied by Río Maullín, the modern Lago Llanquihue spillway. The kame terrace deposited during the youngest advance of the LGM is portrayed along the western and southern rim of Lago Llanquihue with a shaded yellow pattern and yellow background. (For interpretation of the references to color in this figure legend, the reader is referred to the Web version of this article.)

cupressaceous conifers *Fitzroya cupressoides* and *Pilgerodendron uviferum*. The palynomorph *Nothofagus obliqua* type includes the species *N. obliqua, N. alpina,* and *N. glauca*. We calculated running means of selected pollen taxa using a triangular weighing function of values along 7 adjacent levels.

We tallied macroscopic (>106 μm in diameter) charcoal particles to document local fire activity (Whitlock and Anderson, 2003). Macroscopic charcoal was counted from 2-cc sediment samples obtained from 1-cm thick and contiguous sections. The samples were prepared using a standard procedure which involves deflocculation in 10% KOH, careful sieving through 106 and 212 μm-diameter meshes to avoid rupture of individual particles, followed by visual inspection on a ZEISS KL 1500 LCD stereoscope at 10× magnification. We then run time-series analysis to detect local fire events using the CharAnalysis software (Higuera et al., 2009), interpolating samples at constant time intervals based in the median time resolution of the record. We deconvoluted the CHAR signal into a peaks and background component using a lowess robust to outliers smoothing with a 1000-yr window width. We calculated locally defined thresholds to identify statistically significant charcoal peaks or local fires events (99th percentile of a Gaussian distribution).

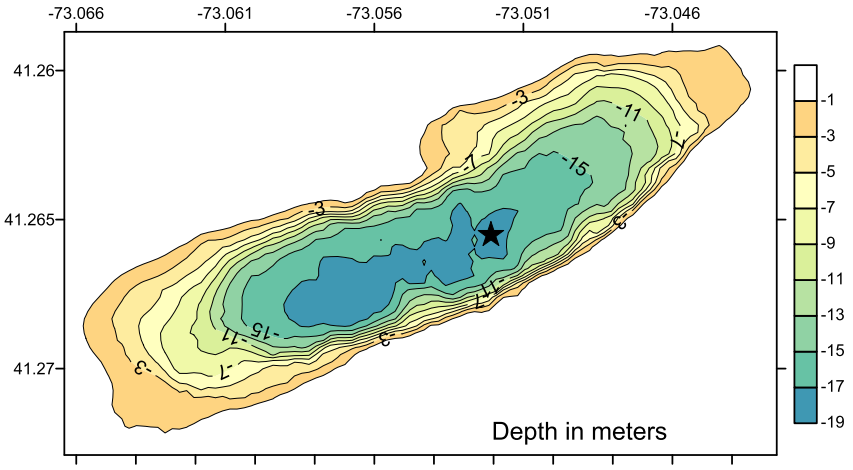

Fig. 3. Bathymetric map of Lago Pichilaguna showing contour lines every 2 m and location of the studied cores (black star).

3. Results

3.1. The sedimentary record

Cores were correlated using lithological markers and magnetic susceptibility to produce a 6.7-m long composite sequence for the deepest water sector (cores from year 2007: 0701SCA and SCB, cores from year 2009: PILA1A-1U-1 to 4, PILA1C-3U-1; and cores from year 2014: 1402AT3) (Fig. 4). The sediment sequence is composed of banded silts grading into laminated mixed clastic and organic silts at the base, laminated diatomaceous and organic oozes in the middle and massive organic oozes at the top. Multiple pyroclastic layers, identified as cryptotephra and tephra, are interspersed throughout the sequence. The most prominent tephra are: a 9-cm thick layer located at 434 cm depth, a 4-cm thick layer at 32 cm depth, a 3-cm thick horizon at 466 cm depth, and a 2-cm thick at 95 cm depth. The thickest layer corresponds to the Lepué tephra, recently characterized as a regional stratigraphic marker in northwestern Patagonia with an age of ~11,000 cal. yr BP by Alloway et al. (2017). The identity and eruptive source of the two tephra beds at 466 and 32 cm depth is current unknown but maybe Calbuco-sourced. These tephra beds have not been preserved or recognized within adjacent equivalent-aged andic soil sequences (Alloway, unpublished material).

Magnetic susceptibility values are moderate (less than 100 SI) in the basal portion (610–670 cm depth), increase to the highest values (almost 300 SI) around 550 cm depth and rapidly decrease to < 20 SI at 520 cm depth (Fig. 4). The values remain low (<10 SI) in most of the upper 500 cm dominated by organic-rich facies. Conspicuous peaks at 520, 400, 240, 170, 150, 95, and 25 cm depth correspond to discrete tephra and pyroclastic layers, which include reworked volcanic material (Fig. 4).

Sediments from the basal interval (560–670 cm depth) have TOC values around 3–4%; TOC increases to ~15% between 560 and 520 cm depth, and then rises to ~25% between 280 and 240 cm (Fig. 4). The upper 240 cm features fluctuations with decreasing and increasing trends reaching maximum values between 60 and 33 cm depth. TIC is <1% in most levels with values below detection limits in many samples from the lower 570-320 cm and the upper 140 cm intervals. Several discrete peaks in TIC occur in the lower

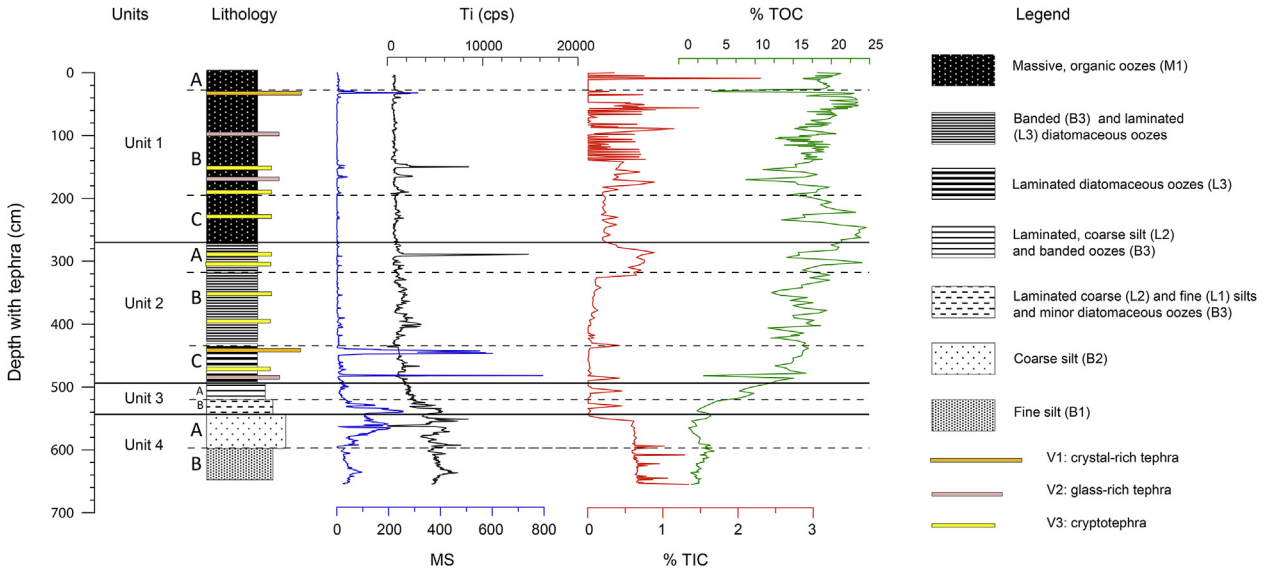

Fig. 4. Lago Pichilaguna stratigraphic column including sedimentary facies, tephra layers, lithological units and profiles of magnetic susceptibility (MS, SI units), Titanium (counts per second), total organic (TOC %) and inorganic (TIC %) Carbon.

half of the sediment sequence. The intervals with the highest TIC content occur at the base of the sequence (623-580 cm depth), the middle (330-280 cm depth) and the top (180-140 cm depth). TIC values in the upper 150 cm are highly variable with some peaks around 90, 70–50 and the top 10 cm depth. TS values are low (<0.5%) with increasing values at the base (623-520 cm depth), decreasing in the middle (520-280 cm depth) and relatively constant in the upper 280 cm (Fig. 4).

The Lago Pichilaguna sedimentary record is composed of three main facies associations: 1) organic with more than 15% TOC, 2) organic-rich with TOC values between 5 and 15%, and 3) clastic with low TOC (<5%).

1. Organic facies association includes facies with more than 15% TOC and they are Massive (M1), Banded (B3) and Laminated (L3) facies. Massive facies (M1) are brown to black, organic oozes with diatoms, TOC ranges between 15 and 25%. TIC values are low, usually less than 0.5%, although with some peaks up to 3%. TS values reach up to 0.5%. Organics are a mixture of macrophyte remains and amorphous organic matter. This facies is interpreted as pelagic sedimentation in distal areas of a lake with high organic productivity and allochtonous organic input, but restricted clastic input from the watershed. Banded facies B3 are greenish organic and diatom–rich fine silts with lower and variable TOC (15–20%) and relatively higher silicate content. The higher silicate composition points to deposition during periods of higher clastic input from the watershed (higher runoff and erosion); relatively higher diatom content also indicates higher diatom productivity relative to other organic sources (macrophytes, littoral aquatic vegetation). Laminated facies are greenish diatomaceous oozes (L3) composed of alternating mm-thick whitish and greenish laminae. Whitish laminae are diatom oozes deposited during blooms and darker laminae are the "baseline" organic and diatomaceous lacustrine deposition. Finely laminated diatomites occur in a variety of lacustrine depositional environments, generally characterized by high diatom productivity, conditions prone to annual blooms and low disturbance processes to ensure preservation of laminae (Bao et al., 2015). This facies association occurs in units 1 and 2 (see below).
2. Organic-rich facies association includes laminated facies (L1, L2) with TOC values between 5 and 15%, and higher silicate content than the previous facies association. L1 facies are finely laminated, darker fine silts. Facies L2 are lighter coarser silts. They group in cm-thick fining upward sequences including sometimes banded organic facies (B3) at top: L2 -> (L1 -> B3). This association occurs in unit 3 and it is interpreted as lacustrine deposition with more intense clastic influence, likely due to higher run-off from the watershed covered with glacial sediments. Fining upward sequences (L2 -> L1; L1 -> B3) indicate alternating periods of higher/lower detrital input into the distal areas of the lake.
3. Clastic facies are banded to faintly laminated gray silts (B1, B2), with high magnetic susceptibility values and silicate content and relatively low TOC (<5%) and diatom content. Darker facies (B1) have higher MS and relatively higher TOC; lighter facies (B2) are usually finer silts with lower MS values. Both facies alternate in cm-thick intervals, but with variable rhythms and frequencies. Some discrete mm-thick light colored laminae (B2) also occur and they are composed of diatomaceous fine silts. The rhythmic nature of the facies and the clastic dominance indicates low organic productivity in the lake, and intense erosional processes in a watershed located on an intermorainal depression and with reduced vegetation cover.

We detect several pyroclastic levels throughout the sequence. Textural properties, smear slide microscope observations and XRF compositional data identify three main volcanic facies: V1: crystal-rich tephra; V2: glass-rich tephra and V3: cryptotephra. V1 and V2 have distinctive boundaries, fining upward textures occasionally showing laminations and high Ti, K and Si. Crystal-rich tephra have higher MS values. Both are interpreted as ash-fall volcanic deposition. V3 have a mixed composition (glass particles, silicate grains, organics, diatoms), diffuse boundaries and usually low MS values. They are interpreted as cryptotephra, representing periods of lacustrine deposition during active volcanic episodes, with a high component of volcanic material transported either as ash fall or as runoff from the watershed.

We identify four main lithologic units based on facies associations (Fig. 4):

Unit 1 (280-0 cm depth) is composed of massive, brownish organic facies M1 with 3 discrete tephra layers and at least 4 clastic layers/cryptotephra. Subunit 1C (280-200 cm) has higher TOC values with a generally decreasing trend (25–20%) and lower TIC values (<0.5%). Subunit 1B (200-30 cm) shows increasing TOC values from 20 to 25% and a higher TIC variability with values up to 1%. The topmost 30 cm (subunit 1A) have lower TOC values and some TIC peaks at the top and relatively higher magnetic susceptibility values.
Unit 2 (503-280 cm depth) features groups of banded diatomaceous organic oozes (B3) and laminated (L3) diatomaceous oozes. Distinct facies changes mark the upper (to massive facies) and lower boundaries (to clastic silts). Subunit 2C (503-445 cm) is dominated by diatomaceous oozes (B3) with higher clastic content, relatively lower TOC and no TIC. Subunit 2B is an alternation of facies B3 and L3. Finely laminated diatomaceous facies (L3) occur in thicker intervals towards the top. The upper subunit 2A (320-280 cm) has relatively higher TOC and TIC values and the lowest TS
Unit 3 (548-503 cm depth) is composed of laminated diatomaceous silts (L1 and L2) with some intervals of banded organic-rich facies B3. MS values are moderate and show a decreasing trend toward the top. TOC values increase from 5 to up to 15%. The base of the unit is an irregular surface, possibly representing a minor unconformity. The lower subunit 3B (548-529 cm) contains two fining upward sequences of laminated, coarser silt (L2) grading into finer, banded, more organic facies B3. The upper subunit 3A (529-503 cm) is an alternation of cm to dm-thick intervals of L2-B3 facies, with some finely laminated finer silts (L1).
Unit 4 (670-548 cm depth) is composed of banded gray silts in cm-to dm-thick layers composed of lighter and finer facies B1 and coarser and darker and with higher MS values facies B2.

3.2. Chronology

The chronology of the Lago Pichilaguna record is constrained by 29 AMS radiocarbon dates obtained from bulk organic samples, assignment of a modern age (−57 cal. yr BP) to the water-sediment interphase, and chronostratigraphic correlation with the Lepué tephra (Alloway et al., 2017) (Table 1). We correlated the onset of sedimentation in Lago Pichilaguna to the basal chronology of the Fundo Llanquihue palynological site (Heusser et al., 1999) (Table 1) considering the absence of suitable material for radiocarbon dating this portion of the Lago Pichilaguna stratigraphy. The correlation rests on the fact that these sites are located 3 km apart along the same ice-proximal side of a prominent ice-contact slope west of Llanquihue Township (Denton et al., 1999b) (Fig. 2). Hence, we

Table 1
Radiocarbon and calibrated dates of the Lago Pichilaguna record, along with the chronology for the correlated Lepué tephra and onset of organic accumulation in the nearby site Fundo Llanquihue (Heusser et al., 1999). Calibration in all cases was performed with calib 7.0.0 using the Southern Hemisphere calibration dataset (McCormac et al., 2004; Stuiver and Pearson, 1993).

Laboratory code	Core code	Original length (cm)	Length with no tephra (cm)	^{14}C yr BP ±1 σ	cal yr BP	2 σ range (cal yr BP)
CAMS-137855	0701SCA	39–40	39–41	460 ± 30	336	490–521
CAMS-137856	0701SCA	48–49	48–50	485 ± 35	344	503–539
CAMS-137857	0701SCA	58–59	58–60	640 ± 35	540	604–650
CAMS-137858	0701SCA	66–67	66–68	655 ± 35	548	605–652
CAMS-137859	0701SCA	87–88	87–89	1160 ± 30	957	1015–1068
CAMS-137860	0701SCB	97–98	90–91	1170 ± 35	937	1019–1161
CAMS-158134	PILA09 1A1U-1	117–118	110–111	1470 ± 30	1289	1326–1369
UCIAMS-122794	PILA09 1A2U1	145–146	138–139	2230 ± 25	2107	2230–2312
CAMS-158135	PILA09 1A2U-1	195–196	188–189	3010 ± 35	2994	3130–3321
UCIAMS-122795	PILA09 1A2U-1	226–227	219–220	3705 ± 25	3894	3988–4087
UCIAMS-122796	PILA09 1A2U-2	285–286	278–279	4685 ± 25	5307	5407–5466
CAMS-158136	PILA09 1A3U-1	330–331	323–324	5745 ± 30	6406	6485–6626
UCIAMS-122941	PILA09 1A3U-1	376–377	369–370	7005 ± 20	7698	7792–7918
UCIAMS-122797	PILA09 1A3U-1	398–399	391–392	7385 ± 25	8029	8139–8287
CAMS-158137	PILA09 1A3U-1	437–438	430–431	8905 ± 35	9774	10,002–10,167
Lepué Tephra	1402AT3-1	441–442	434–435	9800 ± 25	10,925	10,776–11,126
UCIAMS-177595	1402AT3-1	453–454	438–439	10,100 ± 25	11,396	11,580–11,759
CAMS-158138	PILA09 1A4U-1	471–472	456–457	10,785 ± 35	12,671	12,707–12,745
CAMS-158139	PILA09 1A4U-1	501–502	486–487	12,830 ± 45	15,126	15,286–15,519
UCIAMS-177596	1402AT3 -1	507–508	492–493	13,170 ± 30	15,678	15,826–15,999
UCIAMS-177597	1402AT3-1	511–512	496–497	13,555 ± 30	16,171	16,321–16,518
UCIAMS-177598	1402AT3-2	517–518	502–503	13,870 ± 35	16,581	16,801–17,001
UCIAMS-177599	1402AT3-3	522–523	507–508	14,020 ± 35	16,809	17,034–17,219
UCIAMS-177600	1402AT3-4	527–528	512–513	14,195 ± 35	17,112	17,284–17,463
UCIAMS-122798	PILA09 1A4U-1	530–531	515–516	13,980 ± 130	16,525	16,962–17,395
UCIAMS-177601	1402AT3-1	532–533	517–518	14,150 ± 40	17,050	17,227–17,431
UCIAMS-177602	1402AT3-1	538–539	523–524	14,275 ± 45	17,186	17,393–17,568
UCIAMS-177603	1402AT3-2	576–577	561–562	15,575 ± 45	18,715	18,826–18,933
UCIAMS-177604	1402AT3-2	595–596	580–581	16,510 ± 110	19,601	19,912–20,200
UCIAMS-122800	PILA09 1C3U-1	610–611	595–596	16,560 ± 130	19,614	19,974–20,319
Fundo Llanquihue		661–662	646–647	20,650 ± 74	24,532	24,877–25,192

expect ice-free conditions to have started at the same time in both sites. We developed a Bayesian age model for the most recent 20,000 years of the Lago Pichilaguna record using Bacon for R (Blaauw and Christen, 2011) (Fig. 5), and a depth scale that subtracts the thickness of the tephra layers larger than 1-cm thick, considering their geologically instantaneous deposition. The age model suggests continuous deposition of lake sediments in the deepest part of the Lago Pichilaguna basin. Confidence intervals at the 95% value exhibit a median range of 427 years over the last 20,000 years. The chronology of the basal portion of the Lago Pichilaguna record consists of a linear interpolation between the dated 20,000 cal. yr BP level and the chrononostratigraphically correlated base of Fundo Llanquihue at ~25,000 cal. yr BP. We consider the age model spanning the last 20,000 years as robust, and the portion between ~25,000 and 20,000 cal. yr BP as preliminary.

3.3. XRF geochemistry

Variability in the XRF-derived element profiles correspond with changes in sedimentary facies and units (Fig. 6). Ti, Ca and K peaks reflect high content in maphic minerals in tephra and cryptotephra, as well as changes in the minerogenic sediment input from the surrounding watershed. Higher clastic content occurred in unit 4 and the lower part of unit 3. Mineral input is low, but relatively higher in unit 2 than unit 1, dominated by organic deposition (Fig. 4). In lake sequences, several ratios have been used to describe changes in the redox conditions (Fe/Mn), diatom productivity (Si/Ti) and organic productivity (Br/Ti), e.g. Moreno et al. (2007), Frugone-Álvarez et al. (2017). The Fe/Mn ratio in the sediment depends on the redox conditions of the sediment-water interface at the time of deposition, and dominant reducing conditions at the water-sediment interface would enhance dissolution of Mn(II) but not greatly affect Fe(II) leading to higher Fe/Mn values in the sediment (Moreno et al., 2007; Naeher et al., 2013). According to this ratio, more dominant oxidizing conditions occurred in the lower units 3 and 4 and in the upper part of units 2 and 1. The Br/Ti ratio shows similar trends to TOC, with lower values in units 4 and 3, moderate in unit 2 and the highest, with large variability in unit 1. The Si/Ti ratio have relatively lower values in units 4, 3 and 1 and higher in unit 2 and the base of unit 1.

3.4. Palynology

The pollen record from Lago Pichilaguna includes 642 levels and spans the last ~25,000 years, with a median time step of 26 years between adjacent samples (Figs. 7 and 8). We defined 19 pollen zones with the aid of a stratigraphically constrained cluster analysis to facilitate description of the major changes in the pollen record. In the following paragraphs we describe each zone highlighting the three most abundant taxa in decreasing order of mean abundance, their cumulative abundance, their accompanying less-abundant taxa and remarks about the most conspicuous changes of each zone.

- Zone PLG-1 *Nothofagus dombeyi* type-Poaceae-*Isoetes savatieri* (655-622 cm depth, 33 levels, ~25,000–21,800 cal. yr BP). The two most abundant terrestrial taxa account for 93% of the total pollen sum, accompanied by the herbs Asteraceae subfamily Asterioideae (mean: 3%) and traces (mean < 1%) of Apiaceae, *Gunnera, Nassauvia* type, and *Lycopodium magellanicum.* Also present are traces of the conifers *Fitzroya/Pilgerodendron,*

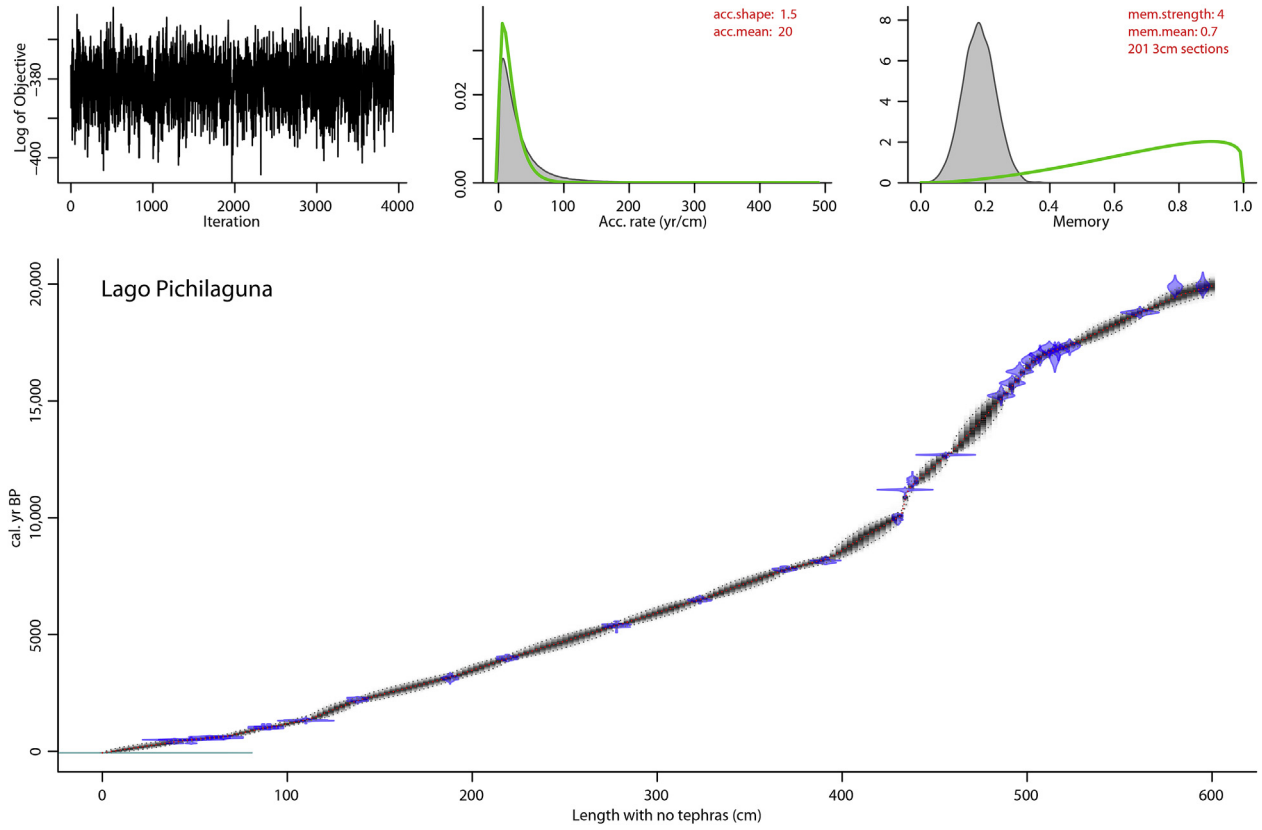

Fig. 5. Age model of the Lago Pichilaguna record spanning the last 20,000 years built using Bacon for R. The probability distribution of the calibrated ages for individual radiocarbon dates are shown in blue. The 95% confidence of the age model is shown in gray, the median probability age of the age model is shown with a red line. The thickness of tephra layers was subtracted for building the age model, considering their instantaneous deposition. (For interpretation of the references to color in this figure legend, the reader is referred to the Web version of this article.)

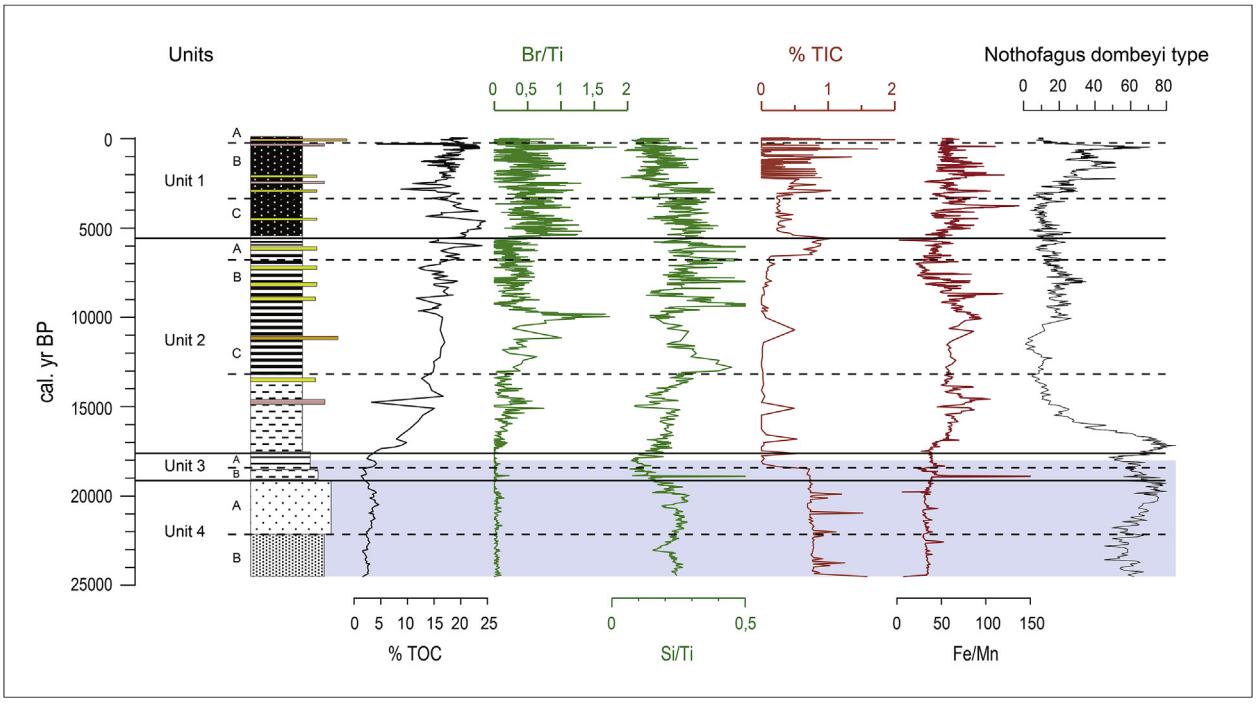

Fig. 6. Facies, sediment composition (TOC and TIC), selected XRF geochemical ratios of the Lago Pichilaguna sequence and lithological units plotted against the age scale (values from tephra layers have been excluded in all profiles). Facies legend similar as Fig. 4. We included the Nothofagus dombeyi type curve to facilitate comparison between the lithological units and the palynology.

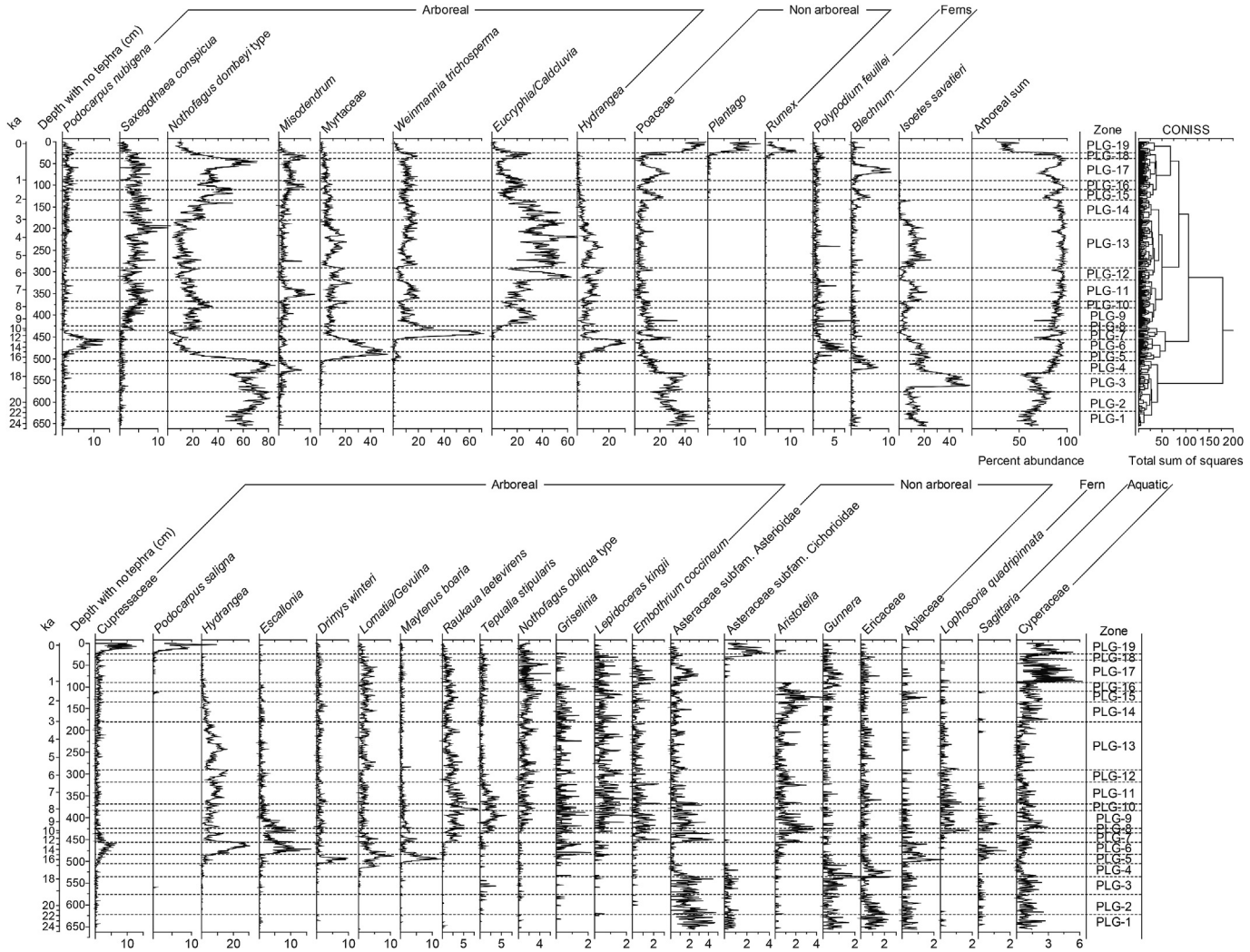

Fig. 7. Pollen percentage diagrams of selected plant taxa from the Lago Pichilaguna record showing the depth with no tephra scale as the primary y axis, the age model scale as secondary y axis, the results of a stratigraphically constrained CONISS ordination, and grouping of plant taxa based on their life forms. The width and scale of individual x axes vary for visual depiction only. The dashed horizontal lines represent the pollen assemblage zone boundaries labelled sequentially from oldest to youngest. The stratigraphically constrained cluster analysis was performed on all terrestrial plant taxa with abundance >2%.

Podocarpus nubigena and *Saxegothaea conspicua*. Arboreal pollen (AP) predominates with an average of 60%.

- Zone PLG-2 *Nothofagus dombeyi* type-Poaceae-*Isoetes savatieri* (622-576 cm depth, 45 levels, 21,800–19,300 cal. yr BP) features an increase in *N. dombeyi* type (from a mean of 57%–70%) and a decline in Poaceae (from a mean of 36% to 24%). The conifers and herbs found in PLG-1 persist in trace abundance while AP increases to a mean of 73%. *Nothofagus* and Poaceae account for 95% of the pollen sum.
- Zone PLG-3 *Nothofagus dombeyi* type-*Isoetes savatieri*-Poaceae (576-535 cm depth, 40 levels, 19,300–17,800 cal. yr BP) features a step increase in *I. savatieri* (from a mean of 24%–33%), concomitant with a major rise in Poaceae (from a mean of 11% to 30%) and declines in *N. dombeyi* type (from a mean of 70% to 62%), Ericaceae. The abundance of Asteraceae subfamily Asterioideae remains unaltered, *Nassauvia* type exhibits a minor increment, and the conifers persist with trace mean abundance. AP declines to a mean of 66%. *Nothofagus* and Poaceae account for 93% of the pollen sum.
- Zone PLG-4 *Nothofagus dombeyi* type-*Isoetes savatieri*-Poaceae (535-505 cm depth, 30 levels, 17,800–16,800 cal. yr BP). Arboreal pollen increases and reaches 90%, driven chiefly by an increase in *N. dombeyi* type (from a mean of 62% to 73%), as all terrestrial and aquatic herbs decline in abundance. The mistletoe *Misodendrum*, the tree *Lomatia/Gevuina* and the fern *Blechnum* show step increases during this zone, coeval with a rapid decline in *I. savatieri* (from a mean of 33% to 19%). *Nothofagus* and Poaceae account for 92% of the pollen sum.
- Zone PLG-5 *Nothofagus dombeyi* type-Myrtaceae-*Isoetes savatieri* (505-484 cm depth, 21 levels, 16,800–15,000 cal. yr BP, 65% of the pollen sum) features a rapid increase in Myrtaceae (from a mean of 1% to 29%), along with diversification of trees (*Fitzroya/Pilgerodendron, Drimys winteri, Maytenus boaria* type, *Escallonia, Lomatia/Gevuina*), appearance of the vine *Hydrangea* and the epiphytic fern *Polypodium feuillei. N. dombeyi* type and Poaceae decline to approximately half their former abundance (from a mean of 73% to 37% and from 16% to 8%, respectively).
- Zone PLG-6 Myrtaceae-*Hydrangea-Isoetes savatieri* (484-456 cm depth, 27 levels, 15,000–12,600 cal. yr BP, 54% of the pollen sum). This zone starts with peak abundance in Myrtaceae (50%) and *Lomatia/Gevuina* (10%), which decline steadily as *Hydrangea*, *Podocarpus nubigena, Fitzroya/Pilgerodendron, Escallonia,*

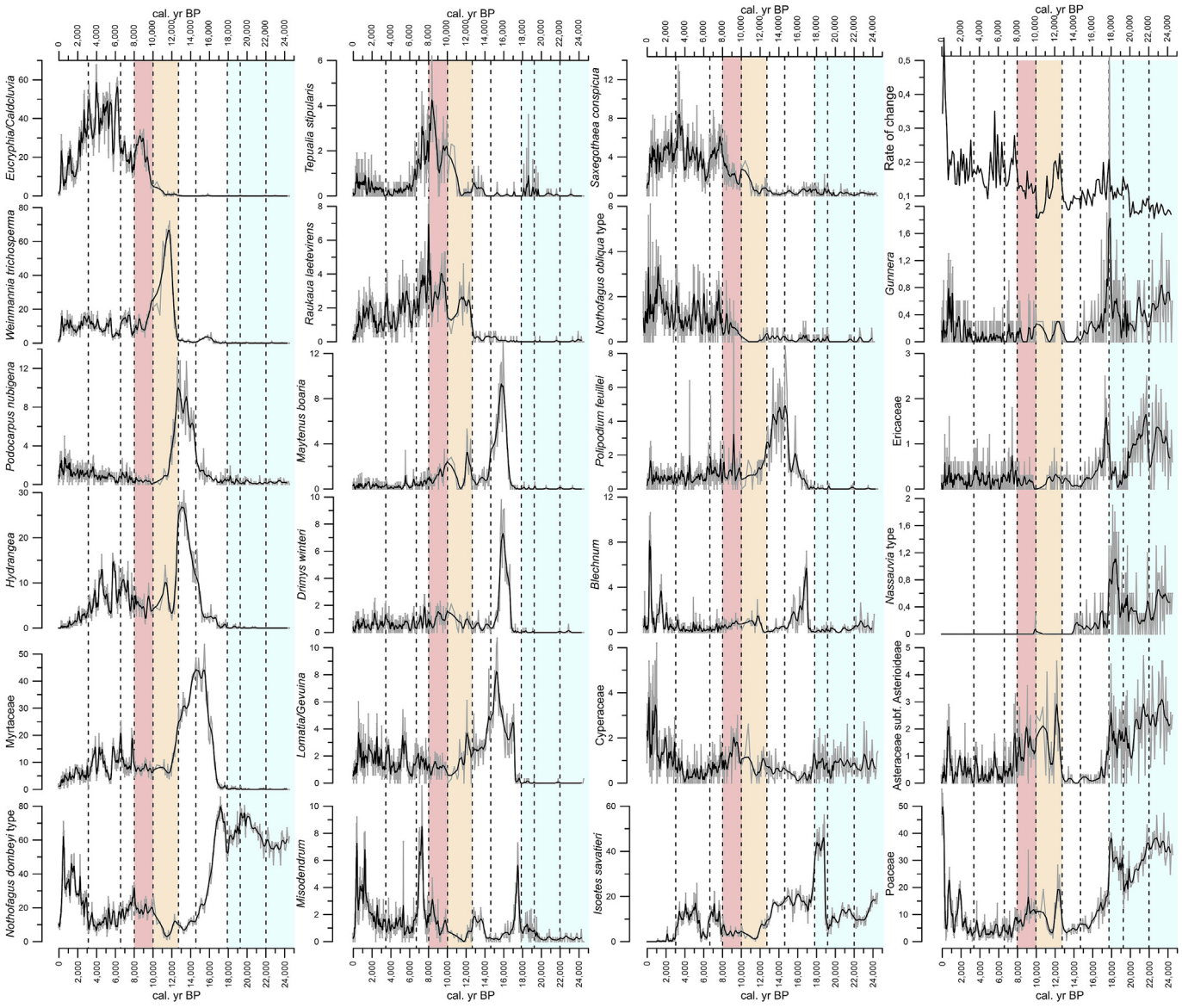

Fig. 8. Selected pollen taxa from the Lago Pichilaguna record expressed in age scale. The raw percentage data are shown in light gray lines, upon which we calculated a weighted moving average shown in black lines. The dashed vertical lines indicate major transitions in the pollen record described and discussed in the main text. The light red vertical rectangles highlights a warm-dry phase during the early Holocene, the light orange ribbon indicates a cold/relatively dry phase at the end of the last glacial termination, the light cyan rectangle comprises the interval corresponding to the last glacial maximum. The upper right diagram shows the rates of change calculation on all terrestrial taxa with abundance >2%. (For interpretation of the references to color in this figure legend, the reader is referred to the Web version of this article.)

Polypodium feuillei and Apiaceae increase and reach their maxima. *N. dombeyi* type declines to a mean of 10%, while arboreal pollen remains high with a mean of 92%. The aquatic *Sagittaria* increases slightly during this zone.

- Zone PLG-7 *Weinmannia trichosperma*-Myrtaceae-Poaceae (456-435 cm depth, 20 levels, 12,600–11,000 cal. yr BP, 65% of the pollen sum) shows a rapid increase in *W. trichosperma* (from a mean of 1% to 45%) associated with declines in all trees, vines and epiphytic ferns. We note that the *W. trichosperma* rise was preceded by a short-lived increment in Poaceae (from 3% to 28%), accompanied by *Embothrium coccineum* and Asteraceae subfamily Asteroideae. The aquatic *Isoëtes savatieri* declines from a mean of 15% to 4%, contemporaneous with the appearance of *Eucryphia/Caldcluvia*, *Raukaua laetevirens* and a minor increase in the fern *Blechnum* type.
- Zone PLG-8 *Weinmannia trichosperma-Nothofagus dombeyi* type-Poaceae (435-424 cm depth, 9 levels, 11,000–9700 cal. yr BP, 54% of the pollen sum) features a prominent decline in *W. trichosperma* (from a mean of 45% to 24%), increases in *N. dombeyi* type (from a mean of 7%–18%), *Embothrium coccineum*, *Raukaua laetevirens* and *Tepualia stipularis,* in conjunction with an increase in *Eucryphia/Caldcluvia* (from a mean of 1% to 6%), the appearance of *Nothofagus obliqua* type, the ferns *Lophosoria quadripinnata* and *Hypolepis*, and low abundance of *I. savatieri.*
- Zone PLG-9 *Eucryphia/Caldcluvia-Nothofagus dombeyi* type-*Weinmannia trichosperma* (424-383 cm depth, 40 levels, 9700-8100 cal. yr BP, 54% of the pollen sum) shows a prominent rise in *Eucryphia/Caldcluvia* (from a mean of 6% to 24%) accompanied by increases in *Saxegothaea conspicua, Raukaua laetevirens*,

Tepualia stipularis and *Lophosoria quadripinnata*, and persistently low levels of *I. savatieri. Nothofagus obliqua* type increases slightly to a mean of 2% and persists in low abundance for the remainder of the record.

- Zone PLG-10 *Nothofagus dombeyi* type-*Eucryphia/Caldcluvia*-Myrtaceae (383-368 cm depth, 15 levels, 8100-7700 cal. yr BP, 55% of the pollen sum). This brief zone shows a decline in *Eucryphia/Caldcluvia* and conspicuous increases in *Saxegothaea conspicua, N. dombeyi* type, Myrtaceae and *Raukaua laetevirens. Isoetes savatieri* rose slightly during this zone.
- Zone PLG-11 Eucryphia/Caldcluvia-Nothofagus dombeyi type-Weinmannia trichosperma (368-319 cm depth, 48 levels, 7700-6400 cal. yr BP, 54% of the pollen sum). Increases are evident in Eucryphia/Caldcluvia, W. trichosperma, Hydrangea and Isoetes savatieri, coupled with declines in Saxegothaea conspicua, N. dombeyi type, Raukaua laetevirens and Tepualia stipularis. Myrtaceae rose from 10% to 25% during a short-lived event near the end of this zone.
- Zone PLG-12 *Eucryphia/Caldcluvia-Nothofagus dombeyi* type-Myrtaceae (319-290 cm depth, 26 levels, 6400-5700 cal. yr BP, 67% of the pollen sum a) features a rapid ~20% increase in *Eucryphia/Caldcluvia* followed by a rapid ~40% decline. Myrtaceae and *Hydrangea* exhibit brief increments during the *Eucryphia/Caldcluvia* decline. *Weinmannia trichosperma* and *Isoetes savatieri* remain in low abundance during this zone.
- Zone PLG-13 *Eucryphia/Caldcluvia-Nothofagus dombeyi* type-*Isoetes savatieri* (290-180 cm depth, 108 levels, 5700-3000 cal. yr BP, 65% of the pollen sum). This interval features preeminence of *Eucryphia/Caldcluvia* (mean: 42%) with 4 large-magnitude (15%–30%) fluctuations that alternate with *Saxegothaea conspicua, N. dombeyi* type and Myrtaceae. A conspicuous increase in *I. savatieri* (from a mean of 3% to 12%) persists over the entire zone. *Weinmannia trichosperma* covaries with *Eucryphia/Caldcluvia* during the largest-magnitude oscillations.
- Zone PLG-14 *Eucryphia/Caldcluvia-Nothofagus dombeyi* type-*Weinmannia trichosperma* (180-134 cm depth, 46 levels, 3000-2000 cal. yr BP, 68% of the pollen sum) features persistent decline in *Eucryphia/Caldcluvia* and a compensatory rise in *N. dombeyi* type, both overprinted by centennial-scale fluctuations. *Isoetes savatieri* shows a decline toward very low values (mean < 1%) which persists until the present, contemporaneous with a rise in Cyperaceae.
- Zone PLG-15 *Nothofagus dombeyi* type-Poaceae-*Eucryphia/Caldcluvia* (134-110 cm depth, 24 levels, 2000-1300 cal. yr BP, 62% of the pollen sum). Poaceae and *Blechnum* type attain maxima early during this zone, followed by peak *N. dombeyi* type abundance, as *Weinmannia trichosperma* and *Eucryphia/Caldcluvia* persist in relatively low abundance.
- Zone PLG-16 *Nothofagus dombeyi* type-*Eucryphia/Caldcluvia-Weinmannia trichosperma* (110-90 cm depth, 20 levels, 1300-1000 cal. yr BP, 66% of the pollen sum). *Eucryphia/Caldcluvia* and *Misodendrum* attain maxima while *N. dombeyi* type, Poaceae and *Blechnum* type remain in low abundance.
- Zone PLG-17 *Nothofagus dombeyi* type-Poaceae-*Weinmannia trichosperma* (90-39 cm depth, 51 levels, 1000-400 cal. yr BP, 66% of the pollen sum). Poaceae and *Blechnum* type attain maxima early during this zone, followed by peak *N. dombeyi* type and *Lomatia/Gevuina* abundance, as *Weinmannia trichosperma* and *Eucryphia/Caldcluvia* persist in relatively low abundance. Cyperaceae attains its maximum abundance during this zone (mean: 6%).
- Zone PLG-18 *Nothofagus dombeyi* type-*Eucryphia/Caldcluvia-Weinmannia trichosperma* (39-25 cm depth, 14 levels, 400-240 cal. yr BP, 65% of the pollen sum). *Eucryphia/Caldcluvia, W. trichosperma* and *Misodendrum* attain maxima while *N. dombeyi* type, Poaceae and *Blechnum* type remain in low abundance. Exotic herbs (*Plantago, Rumex*, Asteraceae subfamily Cichorioideae) appear in the record near the end of this zone.
- Zone PLG-19 Poaceae-*Nothofagus dombeyi* type-*Plantago* (25-0 cm depth, 25 levels, 240 cal. yr BP-present, 67% of the pollen sum) features a prominent decline in arboreal pollen (mean: 53%), the lowest abundance in the entire record, accounted by a rise in Poaceae (from a mean of 10%–45%), and the exotic herbs *Plantago* (mean: 10%), *Rumex* (mean: 5%), Asteraceae subfamily Cichorioideae (mean: 2%). Among the exotic trees, this zone features the appearance of *Pinus* (mean: 1%) and Cupressaceae (mean: 5%).

The rates of change (ROC) parameter (Fig. 8) exhibits values below the mean (0.131 squared chord distance) between ~25,000–20,000, 16,300–12,700 and 11,700–10,000 cal. yr BP, which we interpret as intervals of gradual vegetation change. Values above the mean occur at 19,300 cal. yr BP, between 17,800–17,200 cal. yr BP and almost permanently over the last 10,000 years. We note prominent maxima at 7700, 6400-5600 cal. yr BP and over the last 400 years peaking at 225 cal yr BP (~1725 AD). The latter constitutes the largest peak of the entire record.

3.5. Macroscopic charcoal record

The macroscopic charcoal record from Lago Pichilaguna (Fig. 9) shows very low charcoal accumulation rates (CHAR) prior to 12,800 cal. yr BP, followed by increases between 12,800 and 11,500 cal. yr BP and relatively low values between 11,500 and 10,000 cal. yr BP. Intervals with persistently high CHAR occur between 10,000 and 7700, 5800 and 5400, 4400 and 4200, 3800 and 3600, and between 3200 and 2300 cal. yr BP, alternating with shorter, lower-amplitude increases. A shift to lower values occurs at 2500 cal. yr BP with a prominent peak between 1200 and 900 cal. yr BP.

Time series analysis of the macroscopic charcoal data using CharAnalysis (Fig. 9) reveals 46 fire episodes (statistically significant peaks) and important changes in the low-frequency background signal. Fire episodes are virtually absent between ~25,000 and 15,000 cal. yr BP, except for one event at ~16,500 cal. yr BP. Fire-episode frequency increases from 15,000–2700 cal. yr BP punctuated by millennial-scale declines, the most prominent of which took place between 12,400–10,800 and 7700-7100 cal. yr BP, followed by a decline between 2700 and 1800 cal. yr BP and a final increase at 800 cal. yr BP. The size or magnitude of the fire episodes is high for peaks at 5700, 7800, 7300, 10,000, 1200 and 5200 8400 cal. yr BP. When converted to a logarithmic scale we observe large and intermediate magnitude events during the last 10,000 years, with a distinct clustering of large-magnitude fire episodes at times of peak frequency (Fig. 10). A conspicuous cluster of intermediate-magnitude events occurs between 12,700 and 11,500 cal. yr BP (Figs. 9 and 10).

4. Discussion

The Lago Pichilaguna basin rests on a moraine complex deposited by the Lago Llanquihue glacier lobe during the last glaciation. The lake and moraines are perched above the extensive outwash plains that mantle the lowlands of the Longitudinal Valley of the Chilean Lake District (Fig. 2). Geomorphic, stratigraphic and geochronologic studies indicate that this moraine complex was deposited just before ~26,000 cal. yr BP, during the penultimate expansion of Andean glaciers into the lowlands of the Chilean Lake District during the LGM (Denton et al., 1999b; Moreno et al., 2015).

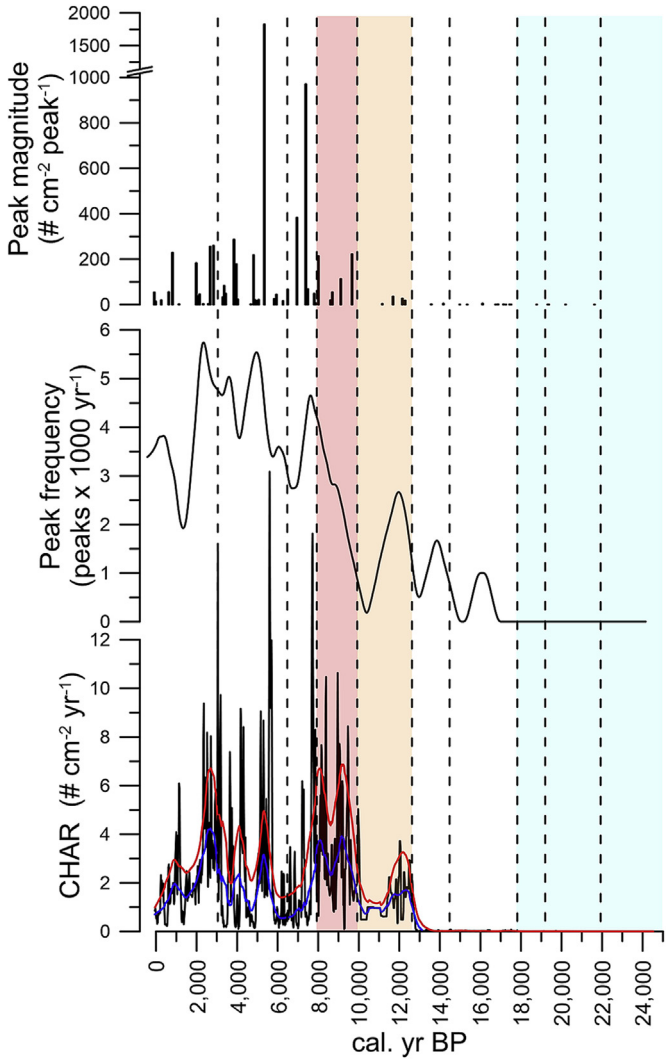

Fig. 9. Macroscopic charcoal record from Lago Pichilaguna and time series analysis using CharAnalysis. The dashed lines and colored ribbons follow the chronology and interpretations shown in Fig. 8.

The youngest LGM advance of the Lago Llanquihue glacier lobe was more restricted in extent and deposited kame terraces at lower elevation on the proximal side of the previously deposited moraines (Fig. 2). Meltwater at the time drained westward through Río Maullín, which runs ~1.6 km south and ~60 m lower in elevation than Lago Pichilaguna (Fig. 1). Hence, Lago Pichilaguna has evolved as a closed-basin lake since the LGM, isolated from glaciolacustrine and glaciofluvial influences related to the youngest LGM advance and the postglacial fluvial network.

4.1. Depositional evolution of Lago Pichilaguna

Sedimentological facies and geochemical proxies define five main stages in the depositional evolution of Lago Pichilaguna: 1) a lake dominated by clastic input prior to 17,800 cal. yr BP; 2) a lacustrine system with low organic deposition (17,800–17,100 cal. yr BP) and increasingly higher organic, diatomaceous sedimentation during the initial stages of T1 (17,100–15,000 cal. yr BP), 3) a lake progressively dominated by organic deposition during the later stages of deglaciation until the early Holocene (15,000–10,200 cal. yr BP), 4) a highly productive lake with some phases of annually laminated diatomaceous oozes during the first half of the Holocene (10,200–5200 cal. yr BP), and 5) a lake dominated by organic deposition since 5200 cal. yr BP and likely with higher lake levels than earlier during the Holocene.

Clastic sediments with high Ti and MS values deposited in Lago Pichilaguna prior to 17,800 cal. yr BP (unit 4) indicate a period of intense erosion of the watershed which is composed of glacial deposits. Alternation of coarser and finer silts in fining upward sequences suggest changes in the intensity of run-off/erosion processes in the watershed. The lake environment remained well oxygenated (low Fe/Mn) with low organic productivity (low TOC and Br/Ti) prior to 17,800 cal. yr BP (Fig. 6).

An increase in organic deposition started at 17,800 cal. yr BP (TOC and Br/Ti), along with a decrease in clastic input to the lake and less dominant oxic conditions at the lake bottom (increasing Fe/Mn) (Fig. 6). These trends indicate a lake environment with higher organic productivity, progressively less dominated by allochtonous sediment input from the watershed. Diatom productivity increased and banded diatomaceous oozes (facies B3) alternated with finer and coarser diatomaceous silts. A rapid decrease in clastic input occurred between 17,800 and 17,100 cal. yr BP, marking a period of lower run-off and erosion in the watershed. Increasing organic productivity occurred between 17,100 and 15,000 cal. yr BP and some TIC peaks suggest short periods of calcite deposition, possibly associated with algal blooms (Fig. 6). Deposition of diatomaceous silts with abundant clastic content (facies L1) marks periods of higher denudation of the watershed (stronger rainfall).

We observe dominance of diatomaceous sediments and an increasing trend in organic productivity at 15,000 cal. yr BP (onset of unit 2), suggesting reduced reworking of glacial sediments from the watershed (Fig. 4). Sediments deposited between 15,000 and 10,200 cal. yr BP (subunit 2C, 503-445 cm) still have a significant clastic component, but organic matter increases and few carbonate peaks also occur. The trend toward increasing organic productivity reached a maximum at 14,500 cal. yr BP followed by a decline until 12,700 cal. yr BP and resumption of the increasing trend after 12,700 cal. yr BP. We lack XRF data to examine the transition into the Holocene, but observe that clastic facies disappear after 10,200 cal. yr BP (onset of subunit 2B), and banded diatomaceous oozes (facies B3) with less clastic content alternate with finely laminated diatomaceous oozes (facies L3). Organic productivity reached a maximum at 9500 cal. yr BP, marked by the highest Br/Ti values of the whole sequence. This peak suggests warm Holocene conditions prior to 8700 cal. yr BP (Figs. 4 and 6).

The interval between 8700 and 6200 cal. yr BP features thicker intervals of finely laminated diatomaceous facies (L3), indicative of high diatom organic productivity, although Br/Ti values declined after the 9500 cal. yr BP maximum. Higher diatom productivity with development of finely laminated facies likely associated to algal blooms correspond with a period of relatively increasing oxic conditions in the lake (lower Fe/Mn) (Fig. 6) suggestive of better mixing of the water column that could be brought by lower lake levels and/or stronger wind activity. Periods of finely laminated diatomaceous oozes occur between 424-419, 390–376, 345–341, 335–321, and 314-301 cm depth that correspond in age to the intervals 8700–8600, 8000–7730, 6845–6725, 6560–6180, and 6024-5700 cal. yr BP (Fig. 6). Alternation of banded B3 and laminated L3 facies occurred in fluctuations at centennial scale between 8700 and 6200 cal. yr BP.

The mid Holocene, between 6200 and 4000 cal. yr BP (subunit 2A, 280–320 cm and subunit 1C), features the highest TOC accumulation in the lake sequence and a progressive transition to more massive, organic-rich facies and the disappearance of periods with finely laminated diatomaceous ooze deposition (Figs. 4 and 6). These features are coherent with relatively higher lake levels and

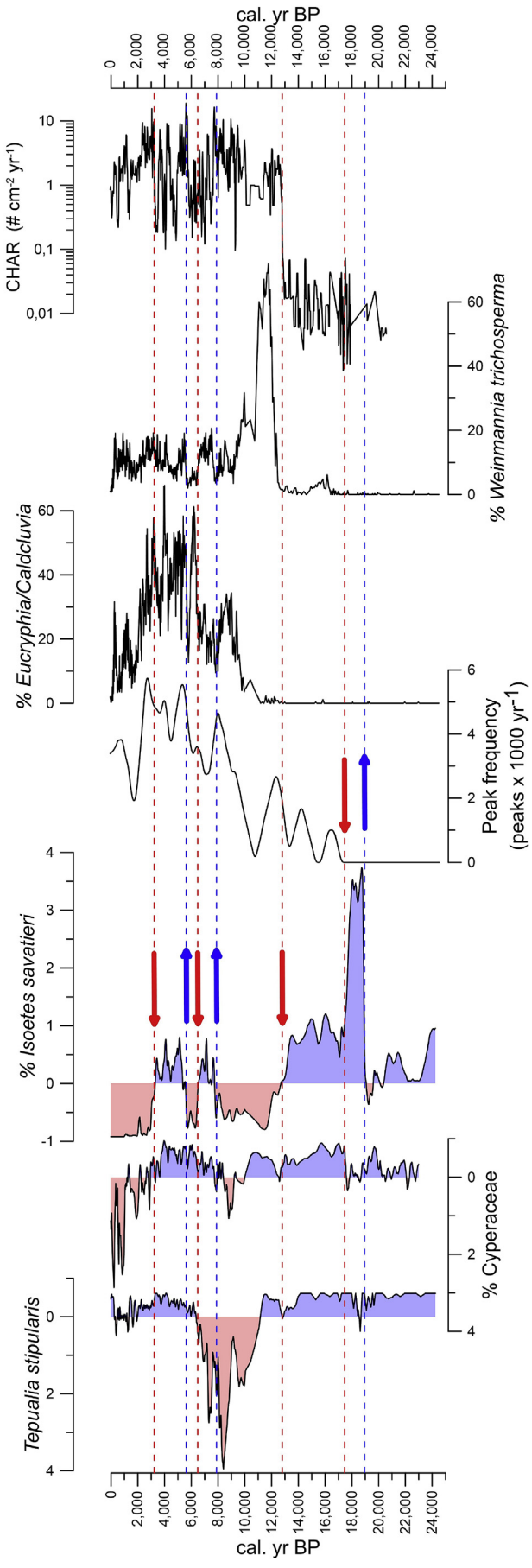

more diverse productivity, not dominated by diatoms. The interval between 6200 and 5200 cal. yr BP is characterized by a progressive increase in reducing conditions (increasing Fe/Mn values) and the presence of some calcite in the sediments.

A new lake depositional stage started at 5200 cal. yr BP with deposition of organic-rich, massive facies M1, an increase in Br/Ti values compared to early and mid-Holocene values, and an increase in more reducing conditions at the bottom of the lake (higher TS, higher Fe/Mn) (Fig. 6). The absence of finely laminated diatomaceous oozes suggest a shift from primary diatom productivity to other algae or macrophytes, responsible for the high organic matter production and high sediment accumulation rates in the lake. TOC increased until 4000 BP when it reached maximum values in the sequence (subunit 1C) coherent with high Br/Ti values and more reducing conditions at the bottom of the lake (higher TS and Fe/Mn) (Fig. 6). Carbonate occurrences were rare during this period. Organic productivity (Br/Ti, TOC) decreased afterwards and reached another low at ~3000 cal. yr BP. TOC levels increased again during the last millennium (1000-300 cal. yr BP). Deposition during the last 300 years shows a small increase in clastic input and decrease in TOC values (subunit 1A) that could reflect an increase in surface runoff due to the Chilean-European deforestation and changes in land use (Fig. 6).

4.2. Vegetation and climate change

The Lago Pichilaguna pollen record allows examination of vegetation changes from centennial to multimillennial to centennial timescales since ~25,000 cal. yr BP (Figs. 7 and 8). The LGM record includes 118 samples which show abundant arboreal pollen with dominance of *Nothofagus* (zones PLG 1-3, mean ± SD: 64 ± 8%), between ~25,000 and 17,800 cal. yr BP, accompanied by traces of its hemiparasite *Misodendrum* (mean: 0.5%) and the conifers *Fitzroya/Pilgerodendron* (mean: 0.1%), *Podocarpus nubigena* (mean: 0.3%) and *Saxegothaea conspicua* (mean: 0.3%). The absence of other trees, vines, and epiphytes characteristic of mesic, mid-elevation North Patagonian rainforest (NPRF) suggests an interface between high-elevation species-poor *Nothofagus*-dominated Subantarctic forests and alpine meadows in Andean sectors adjacent to Lago Pichilaguna. In fact, this LGM interval features the highest abundance of herbs, shrubs, ferns, and lycopods (Poaceae, Asteraceae, Apiaceae, Ericaceae, *Gunnera, Nassauvia* type, *Lycopodium magellanicum*) in the entire record, taxa which today are most abundant in barren, open ground environments above and in the interface with the Andean treeline (Figs. 7 and 8). Our results and interpretations are coherent with a recent study of surface pollen samples from high elevation environments in the adjacent Andes of Argentina (Iglesias et al., 2016). Because species of the genus *Nothofagus* produce large quantities of pollen grains susceptible to long-distance transport, we interpret a landscape consisting of cold-tolerant herbs and scattered *Nothofagus* populations with varying degrees of openness during the LGM. Considering that the alpine treeline in the study area today is located at ~1300 m.a.s.l., we infer a treeline lowering of at least 1000 m between ~25,000

Fig. 10. Standardized abundance of Isoetes savatieri, Cyperaceae and Tepualia stipularis relative to their respective mean for the entire Lago Pichilaguna record. The red filling represents anomalies interpreted as indicative of low lake levels, blue filling denote intervals interpreted as high lake levels. Also shown are the percent abundance of Eucryphia/Caldcluvia, Weinmannia trichosperma and the macroscopic Charcoal Accumulation Rate (CHAR) record from Lago Pichilaguna. The dashed vertical lines highlight major transitions in inferred hydroclimate conditions, the red lines denote drying conditions (toward the present) accompanied with a downward pointing arrow, the blue lines and arrows the opposite. (For interpretation of the references to color in this figure legend, the reader is referred to the Web version of this article.)

and 17,800 cal. yr BP.

Within the LGM we recognize an interval with relatively low *Nothofagus* abundance between ~25,000 and 22,000 (zone PLG 1, mean: 57%), a rise between 22,000 and 19,200 (zone PLG 2, mean: 70%), and a decline between 19,200 and 17,800 cal. yr BP (zone PLG-3, mean: 62%) (Figs. 7 and 8). We interpret these changes as variations in the density of glacial *Nothofagus* populations driven by millennial-scale shifts in the regional treeline, ultimately controlled by temperature changes. Hence, we interpret a warming trend that started at 22,000 cal. yr BP and peaked at 19,200 cal. yr BP, followed by sustained cooling until 17,800 cal. yr BP. The predominance of clastic sedimentation between ~25,000 and 17,800 cal. yr BP (Figs. 4, 6 and 11) suggests reworking of the Llanquihue moraines associated to intense runoff in a sparsely vegetated terrain. Furthermore, the increase in MS and high Ti content in the sediments between 19,200 and 17,800 cal. yr BP indicates an intensification of runoff and erosion processes during the extreme cold/wet phase (Figs. 6 and 12).

Nothofagus rose from 48% to 85% between 17,800 and 17,200 cal. yr BP along with *Lomatia/Gevuina, Misodendrum* and the fern *Blechnum*, followed by a sudden appearance of Myrtaceae and Cupressaceae at 16,800 cal. yr BP, along with the trees *Drimys winteri, Maytenus boaria*, the vine *Hydrangea* and the epiphytic fern *Polypodium feuillei* (zone PLG-4, Figs. 7 and 8). These data suggest a rapid increase and diversification of relatively thermophilous species currently present in mesic NPRF, coeval with decreases in cold-tolerant herbs. This change was preceded by the spread of opportunistic, shade-intolerant tree taxa (*Nothofagus, Drimys, Lomatia/Gevuina*) that commonly occupy recently deglaciated or disturbed terrains, marking the onset of forest establishment after the LGM. The ROC parameter (Fig. 8) shows high values during the *Nothofagus* rise between 17,800 and 17,200 cal. yr BP, indicating that this transition stands out as an abrupt event during the LGM to T1 transition. We interpret that rapid warming at 17,800 cal. yr BP led to an abrupt increase in NPRF trees, vines and ferns, marking the onset of T1 in the lowlands of northwestern Patagonia. These changes are contemporaneous with a rapid decrease in clastic input between 17,800 and 17,100 cal. yr BP, indicated by MS and geochemistry, marking a period of decreased run-off and erosion in the watershed, driven by the densification of upland vegetation and of increasing organic productivity in the lake.

Closed-canopy rainforests, similar in composition to modern NPRF, established near Lago Pichilaguna between 17,800 and ~14,800 cal. yr BP with the trees Myrtaceae, *Lomatia/Gevuina* and *Escallonia,* and the epiphytic *Hydrangea* and *Polypodium feuillei* (zones PLG-4 and PLG-5, Figs. 7 and 8), contemporaneous with peak productivity in the lake (Fig. 6). This was followed by increases in the cold-tolerant hygrophilous conifers *Podocarpus nubigena* and Cupressaceae (*Fitzroya cupressoides* and/or *Pilgerodendron uviferum*) at the expense of thermophilous trees between 14,800 and 12,700 cal. yr BP (zone PLG-6), and was coeval with a decline in organic productivity in the lake. We interpret these changes as a shift toward cooler conditions and increased moisture. A rapid increase in *Weinmannia trichosperma* (~70% rise between 12,700 and 11,900 cal. yr BP, zone PLG-7) and Poaceae ensued, contemporaneous with increases in *Embothrium coccineum, Lomatia/Gevuina, Raukaua laetevirens*, Poaceae (possibly the bamboo *Chusquea*), Asteraceae and macroscopic CHAR (Figs. 7 and 8). The correspondence between this floristic turnover and a sudden increase in macroscopic charcoal suggests stand-replacing fires near the study site between 12,700 and 11,900 cal. yr BP (Figs. 9 and 10). Because dense biomass was present at the time (>92% arboreal pollen), and wildfires in these rainforests are limited by ignition sources and fuel desiccation (Holz et al., 2012), we infer a precipitation decline and/or increased precipitation variability commencing at 12,700 cal. yr BP. The ROC parameter shows values above the mean between 12,700 and 11,700 cal. yr BP, indicating that the response of the vegetation to fire disturbance during T1 was abrupt (Fig. 8).

Pollen percentages of *Eucryphia/Caldcluvia* and *Nothofagus dombeyi* type increased at 11,300 cal. yr BP along with those of *Raukaua laetevirens, Tepualia stipularis, Escallonia, Lophosoria quadripinnata,* Poaceae and Cyperaceae following major declines in *W. trichosperma* and *P. nubigena* (zones PLG-8, PLG-9) (Figs. 7 and 8). *Eucryphia/Caldcluvia* and *Tepualia stipularis* achieved high abundance between ~9000 and 8000 cal. yr BP in the context of low abundance of *I. savatieri* and an increase in the frequency and magnitude of local fires (Figs. 7–10). The species *T. stipularis* commonly thrives in sectors with impeded drainage, even growing partially submerged along the littoral zone of northwestern Patagonian lakes; hence we interpret the increase of *T. stipularis* as a centripetal shift of littoral environments driven by lake-level lowering between 11,300 and 7700 cal. yr BP. This explanation also applies to the macrophyte Cyperaceae (Figs. 7, 8 and 10), which commonly inhabits the periphery of lakes. Altogether these data indicate a floristic turnover with dominance of the thermophilous Valdivian rainforest (VRF) tree *Eucryphia/Caldcluvia,* disappearance of the cold-tolerant *P. nubigena*, enhanced fire activity and lower lake level, thus suggesting warm and dry conditions between 11,300 and 7700 cal. yr BP. The deciduous tree *Nothofagus obliqua* type appears in the record at ~10,000 cal. yr BP and persists in low abundance until the present, suggesting that lowland deciduous forests established in sectors of the Longitudinal Valley just north of Lago Pichilaguna and that their southern limit remained stable during the Holocene.

Eucryphia/Caldcluvia pollen shows a ~20% decline starting at 8700 cal. yr BP (zone PLG-9), followed by increases at 7700, 7200, and 6500 cal. yr BP and led to a plateau in pollen abundance between ~6400 and 2700 cal. yr BP (zones PLG 12–14, mean: 42%) (Figs. 7 and 8). Within this plateau we identify rapid increases starting at 5700, 5200, 4200, 3400 and 2800 cal. yr BP that led to centennial-scale maxima, followed by a sustained decline punctuated by increases at 2600, 2200, 1300 and 400 cal. yr BP. Local fire frequency achieved millennial-scale maxima between 6800 and 6000, 5400 and 5000, 4000 and 3500, 3000 and 2400, 1200 and 300 cal. yr BP with predominance of large-magnitude events (Figs. 9 and 10). The ROC parameter (Fig. 8) shows multiple large-magnitude peaks associated with the discrete increases in *Eucryphia/Caldcluvia* and charcoal, the largest of which occurred at 7700 and 5600 cal. yr BP, suggesting that local fires may have acted as a catalyst of vegetation change during the last 8000 years. *Nothofagus* started a rising trend at 3100 cal. yr BP and achieved successive maxima at 2300, 1600, 1300, and 500 cal. yr BP that follow the *Eucryphia/Caldcluvia* peaks (Figs. 7 and 8). Cyperaceae shows a similar multi-millennial trend over the last 3000 years (zones PLG 14–18). *I. savatieri* rose and achieved high levels ($\geq$9%) between 7800–6500 and 5700-3300 cal. yr BP and low abundance between 6500 and 5700 cal. yr BP ($\leq$5%) and during the last 3300 years ($\leq$3%).

Finally, we observe an abrupt increase in Poaceae at ~260 cal. yr BP and peak fire frequency (zone PLG-19), followed by high percentages of Cupressaceae (probably introduced species of the genus *Cupressus*), *Pinus*, and the herbs *Rumex, Plantago,* Asteraceae subfamily Cichorioidae and Cyperaceae (Figs. 7 and 8). These changes were contemporaneous with sharp declines in *Eucryphia/Caldcluvia, Weinmannia trichosperma, Saxegothaea conspicua, Tepualia stipularis* and a ~50% lowering in arboreal pollen relative to the 1000-300 cal. yr BP interval. The ROC parameter (Fig. 8) shows that the magnitude and rapidity of these vegetation changes were extraordinarily fast, representing the largest rate of change in the entire ~25,000-year long record. Our data indicate rapid

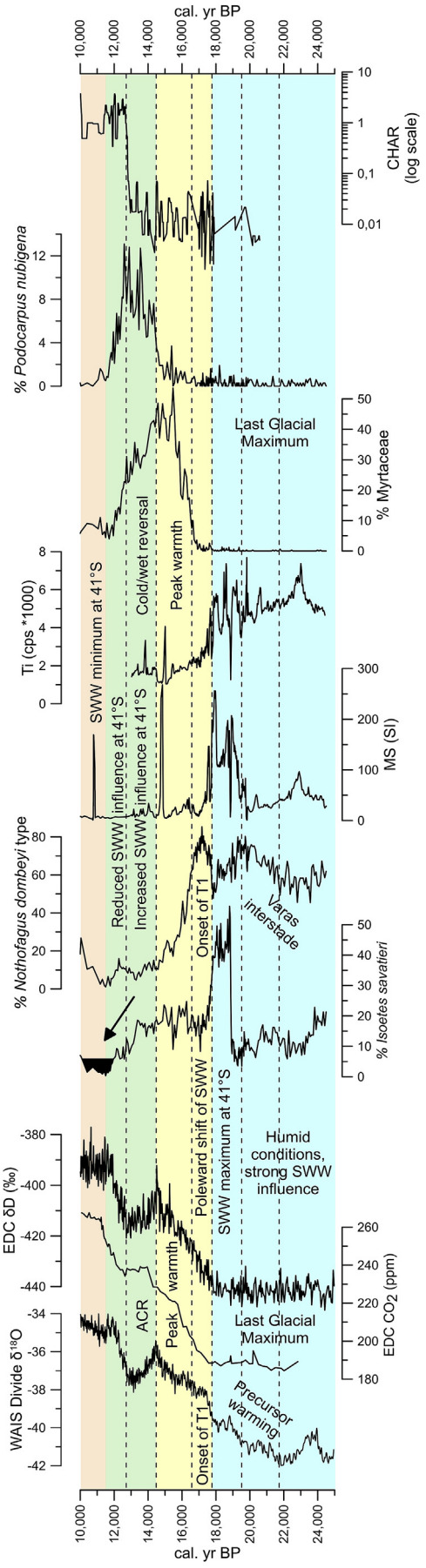

deforestation driven by fire beginning at ~450 cal. yr BP (confidence interval: 500-330 cal. yr BP), establishment of pastures and spread of exotic species introduced by Chilean-European settlers (Figs. 7 and 8).

4.3. Hydrologic inferences

The macrophyte *Isoetes savatieri* is an obligate aquatic lycopsid that inhabits shallow environments, normally <5 m depth, in freshwater lakes of central and southern Patagonia (Hickey et al., 2003). Its maximum growth depth is limited by water turbidity which limits light penetration, most notably in relatively shallow eutrophic lakes. Hence, variations in the abundance of *Isoetes savatieri* in the palynological record from the relatively shallow and turbid Lago Pichilaguna can be used as a diagnostic for changes in the extent and/or proximity of shallow littoral environments to the coring site through time which, in this study, corresponds to the deepest part of the lake. We standardized the percent abundance of *I. savatieri* to the mean of the entire record and identified positive anomalies which alternate with negative anomalies (12,600–7700, 6600–5600, and 3200-0 cal. yr BP) (Fig. 10). Negative anomalies in *I. savatieri* between 11,300 and 7700 cal. yr BP were contemporaneous with high levels in the summer-drought resistant thermophilous VRF tree *Eucryphia/Caldcluvia*, positive anomalies in the littoral Cyperaceae and peak frequency and magnitude of local fires (Figs. 7, 8 and 10), along with declines in hygrophilous cold-tolerant NPRF conifers (Figs. 7 and 8). This contrasts with positive anomalies during an interval dominated by hygrophilous NPRF species between 17,500 and 12,700 cal. yr BP mentioned above, featuring low Cyperaceae and absence of local fires (Figs. 7, 8 and 10). The largest positive anomalies in *I. savatieri* occurred between 19,000 and 17,800 cal. yr BP, and were contemporaneous with abundant *Nothofagus* along with a major increase in Poaceae and other herbs commonly found in alpine environments (Figs. 7, 8 and 10), which we interpreted as an arboreal decline driven by extreme glacial climate during the final LGM stade. From these comparisons we note a correspondence between the sign of hydrologic balance inferred from the terrestrial pollen record and *I. savatieri* abundance, which we attribute to past lake-level fluctuations. Positive hydrologic balance (precipitation > evaporation) leads to higher lake levels and inundation of extensive flatlands in the periphery of Lago Pichilaguna, increasing the areas susceptible for occupation of this shallow-water macrophyte. Negative hydrologic balance (evaporation > precipitation) leads to lower lake levels and a reduction in the shallow, gentle-sloping habitats adequate for the occurrence of *I. savatieri*. From this discussion we interpret high lake levels between ~25,000 and 12,700 cal. yr BP with a rapid rise that led to a maximum between 19,000 and 17,800 cal. yr BP, a sudden decline between 13,000 and 12,700 cal. yr BP and low levels between 12,700 and 7700 cal. yr BP (in particular between 11,000 and 8000 cal. yr BP) (Fig. 10).

Isoetes savatieri increased and reached positive anomalies between 7700 and 3200 cal. yr BP (Fig. 10), suggesting a high lake-level stand, which was punctuated by a negative anomaly between 6600 and 5600 cal. yr BP and followed by persistently negative anomalies over the last 3200 years. Similarities in timing and direction between the abundance of *I. savatieri* microspores and hygrophilous NPRF conifers (mainly *Saxegothaea conspicua* but also *Podocarpus nubigena*) (Figs. 7 and 8) suggest coherent changes in terrestrial and aquatic ecosystems in response to a common driver, i.e. changes in precipitation. A shift from finely laminated

Fig. 11. Comparison of selected pollen taxa from the Lago Pichilaguna record with ice core data from Antarctica over the interval between ~25,000 and 8000 cal. yr BP.

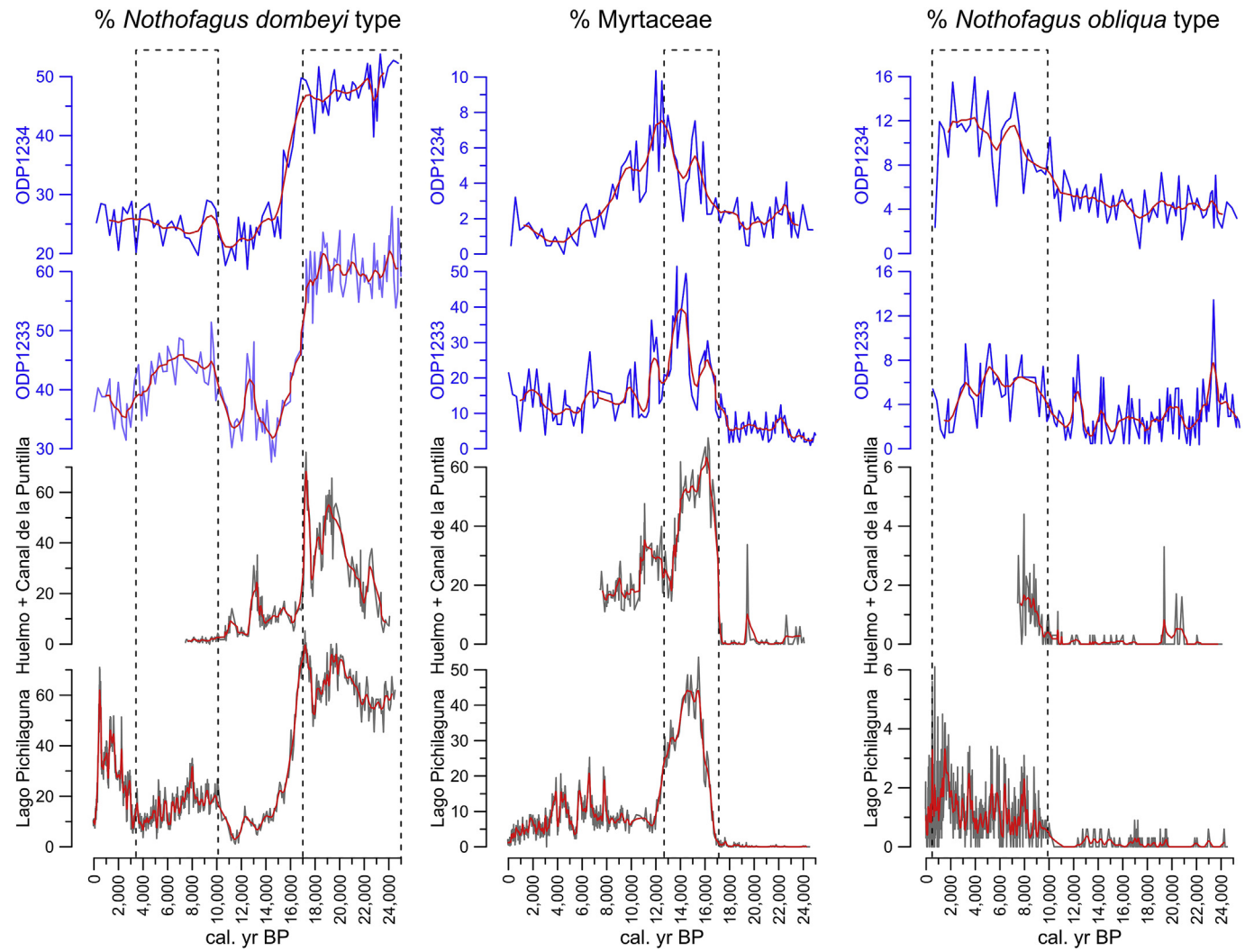

Fig. 12. Comparison of selected pollen taxa from the Lago Pichilaguna record with the Canal de la Puntilla + Huelmo spliced pollen record and ODP sites 1233 and 1234. The blue lines indicate the raw percent abundance in the marine records, the gray line the same but in the continental records. The red lines represent running weighted means in each record. The dashed vertical rectangles highlight shared aspects of the stratigraphy of each taxon: (i) in the case of Nothofagus dombeyi type the vertical rectangles show the high abundance during the LGM and a subsequent increase during the Holocene, (ii) in the case of Myrtaceae the rectangle constrains a major increase to peak abundance during T1, and (iii) in the case of Nothofagus obliqua type it shows an increase over the last 10,000 years. (For interpretation of the references to color in this figure legend, the reader is referred to the Web version of this article.)

diatomaceous oozes during the early Holocene to massive organic-rich facies at ~6200 cal. yr BP (Figs. 4 and 6) provides an independent indication for a lake-level rise, consistent with the palynologicaly based increase in precipitation.

An apparent mismatch in hydroclimate signals is evident when comparing the increased abundance of *Eucryphia/Caldcluvia* between 8000 and 3000 cal. yr BP and the palynological/sedimentological changes discussed in the previous paragraph. Clues to resolving this apparent incongruence include the autoecology of *Eucryphia cordifolia* (one of the two species incorporated into the palynomorph *Eucryphia/Caldcluvia*) and the fire history over this interval. On one hand, *E. cordifolia* is a summer-drought tolerant, thermophilous, fast-growing, shade-intolerant tree that rapidly colonizes disturbed terrains, thanks to its high seed production (Donoso Zegers, 2006) and capacity to resprout (Gonzalez et al., 2002). According to Jara and Moreno (2014) low-elevation forest communities dominated by *Eucryphia cordifolia* in the Longitudinal Valley of the Chilean Lake District could represent early or intermediate successional stage after periodic catastrophic disturbances, analogous to the forest communities dominated by *Nothofagus* at middle and high elevation (>400 masl) in the Andes (Veblen and Ashton, 1978). On the other hand, the stratigraphy of macroscopic charcoal shows maximum frequency of local fires between ~8000 and 3000 cal. yr BP. We posit that disturbance by fire drove compositional changes in terrestrial ecosystems, favouring *Eucryphia/Caldcluvia* during a predominantly cool-wet multi-millennial interval since ~8000 cal. yr BP. This took place during an interval characterized by the establishment of a vegetation mosaic featuring NPRF and VRF species with contrasting physiological tolerances (Moreno, 2004). During the last ~3000 years we observe a correspondence between increases in *Eucryphia/Caldcluvia* and local fires, followed by increases in Poaceae and *Blechnum*, and subsequent increases in *Nothofagus* pollen (Figs. 7 and 8). We will discuss these changes in the final subsection titled “Paleoclimate implications II: the last 8000 years”.

4.4. Paleoclimate implications I: from ~25,000–8000 cal. yr BP

The Lago Pichilaguna record suggests a ~1000 m lowering in the regional treeline during the LGM, which translates into ~6.5 °C cooling using an adiabatic lapse rate of 0.65 °C/100 m, coupled with enhanced precipitation. This estimate agrees with Denton et al. (1999a)'s interpretation of a ~1000-m snowline lowering during the LGM based on the extent of Andean glaciers in the lowlands of the Chilean Lake District relative to the modern equilibrium line altitude, and previous estimates based on palynological studies in the same region (Heusser et al., 1999; Moreno et al., 1999). Within the ~25,000 to 17,800 cal. yr BP interval we identify a rise in arboreal pollen between 22,000 and 19,200 cal. yr BP that takes place during the Varas interstade (Mercer, 1972), followed by rapid cooling and increase in precipitation between 19,200 and 17,800 cal. yr BP (Moreno et al., 2015) (Fig. 11). The latter was contemporaneous with the youngest advance of Andean ice lobes into the lowlands of northwestern Patagonia during the LGM (Denton et al., 1999b). Our results replicate the Canal de la Puntilla + Huelmo spliced pollen record, also located in the Longitudinal Valley, which shows very low *Nothofagus* values prior to ~22,000 cal. yr BP (mean: 18.3%) followed by a multi-millennial rise and a subsequent reversal between 19,400 and 17,800 cal. yr BP (Moreno et al., 2015) (Fig. 11). High precipitation in northwestern Patagonia suggests a strong influence of the SWW between ~25,000 and 17,800 cal. yr BP, this influence increased and reached its maximum during the youngest LGM advance of glaciers in northwestern Patagonia (19,400–17,800 cal. yr BP). Comparison of our Lago Pichilaguna data with the pollen records from marine cores ODP 1233 (Heusser et al., 2006b) (41°10′S, 74°13′W, 838 m water depth) and 1234 (36°11′S, 73°14′W, 1015 m water depth) (Heusser et al., 2006a) reveals a common *Nothofagus dombeyi* type-dominated assemblage (mean: 65%, 60%, and 48%, respectively) between ~25,000 and 17,500 cal. yr BP (Fig. 12), indicating that *Nothofagus* trees were ubiquitous in northwestern Patagonia during the LGM. The pervasive occurrence of cold-tolerant hygrophilous trees during the LGM has been attributed to the prevalence of hyperhumid conditions, which also suppressed the entrainment and transport of airborne particles (sands and loess) from the outwash plains extending westward from the glacial lobes (Alloway et al., 2018).

Glacial climate and expanded glaciers in northwestern Patagonian correlate with cold temperatures, low atmospheric CO_2 concentrations, high dust concentrations in Antarctic ice cores until ~18,000 cal. yr BP(Lambert et al., 2012; Monnin et al., 2001; Stenni et al., 2010), and the commencement of a sustained and irreversible warming trend in the δD and the $\delta^{18}O$ records from the EDC and WDC Antarctic ice cores at ~18,000 cal. yr BP, respectively (Fig. 11). The WDC record also shows a gradual warming between ~22,000 and 19,000 cal. yr BP which halted between ~19,000 and 18,000 cal. yr BP (WAIS Divide Project Members, 2013). The magnitude and rate of this event fall well within LGM changes in the same record (see for example the interval between 30,000 and 24,000 cal. yr BP), and is attributed to a circum-Antarctic sea-ice decline driven by local insolation (WAIS Divide Project Members, 2013). This intra-LGM Antarctic warming overlaps in timing with the Varas interstade, and its end correlates with the final cooling phase during the LGM in northwestern Patagonia (Fig. 11). These contemporary changes raise the possibility that insolation-driven sea ice shrinkage in the Southern Ocean triggered temperature increases in the mid and high southern latitudes and a poleward shift of the SWW during the LGM, followed by stabilization of sea ice, northward-shifted SWW and persistence of cold conditions during the youngest LGM advance of glacier lobes in northwestern Patagonia.

The *Nothofagus* rise at 17,800 cal. yr BP in the Lago Pichilaguna record marks a rapid onset of T1 and was contemporaneous with other palynological sites in the region, collapse of multiple ice lobes throughout Patagonia and New Zealand's South Island (Moreno et al., 2015), as well as sustained increases in temperature and atmospheric CO_2 concentration revealed by Antarctic ice cores (Monnin et al., 2001) (Fig. 11). Because this event was coeval with a lake-level decline in the Lago Pichilaguna record, we interpret a southward shift of the SWW at the commencement of T1. Our results replicate the conclusions shown by Moreno et al. (2015), who inferred a reduction in precipitation at the beginning of T1 based on the disappearance of Magellanic Moorland species from the lowlands of the Chilean Lake District. A poleward shift of the SWW may have invigorated deep upwelling in the Southern Ocean which, in turn, boosted diatom productivity (Andersen et al., 1999) and CO_2 degassing from the deep ocean, establishing a positive feedback on the deglacial warming trend during the early stages of T1.

Large-scale warming led to the establishment of diverse closed-canopy North Patagonian rainforests including thermophilous trees, vines and epiphytic ferns between 16,800 and 14,400 cal. yr BP. This shift was rapid (Fig. 8) and synchronous with the Canal de la Puntilla + Huelmo spliced pollen record (Moreno et al., 2015), and within dating errors and marine reservoir-age uncertainties with the ODP 1233 and 1234 records (Heusser et al., 2006a, 2006b) (Fig. 12), demonstrating the regional significance of this event. Our data from Lago Pichilaguna indicate that peak deglacial warmth was achieved within ~1200 years following the onset of T1, in agreement with palynological records and rapid deglaciation deep into the Andes of northwestern Patagonia shown in Moreno et al. (2015). Paleoclimate records from Antarctic ice cores, on the other hand, show a more gradual trend to reach the same point, ~3500 years (from ~18,000 to ~14,500 cal. yr BP) (Monnin et al., 2001). Hence, a large portion of the total temperature recovery through the last glacial to interglacial transition in the southern mid- and high-latitudes was accomplished within 1000–3500 years following the onset of T1, feature that contrasts with the abrupt Bolling warming in the Northern Hemisphere (~14,500 cal. yr BP), a quasi-total nearly instantaneous shutdown of Atlantic Meridional Overturning circulation (AMOC) and persistence of extreme cold conditions in the North Atlantic region during the Mystery Interval (~17,500 to 14,500 cal. yr BP) (Denton et al., 2006).

A reversal in warming trend occurred at 14,800 cal. yr BP with a two-phase cooling event that lasted until ~11,000 cal. yr BP. Its initial phase, between 14,400 and 12,700 cal. yr BP, features cold/wet conditions and correlates with the Antarctic Cold Reversal, a halt in the deglacial CO_2 rise (Fig. 11), a southern mid-latitude *trans*-Pacific glacial glacier readvance (Sagredo et al., 2018), a decline in diatom productivity in the Southern Ocean, invigorated AMOC and Northern Hemisphere warming. The second phase, between 12,700 and 11,000 cal. yr BP, features persistence of low temperature and a decline in SWW-derived precipitation which correlates with renewed warming and CO_2 rise in Antarctic ice cores (Fig. 11), glacial recession and stabilization throughout Patagonia and the Southern Alps from New Zealand, a halt in AMOC and cooling in vast sectors of the Northern Hemisphere during the Younger Dryas stadial (Moreno et al., 2015).

Holocene starts with warm conditions and low lake level in the Lago Pichilaguna record between 11,000 and 8000 cal. yr BP (Figs. 10 and 11), in agreement with previous studies from northwestern Patagonia which show terrestrialization of shallow lakes or lake regressive phases over that interval (Abarzua et al., 2004; Moreno and Leon, 2003; Moreno and Videla, 2016; Pesce and Moreno, 2014). The sediments from Lago Pichilaguna show a rising trend in organic productivity that peaked at 9500 cal. yr BP,

most likely driven by high temperatures and low lake levels. Warm and dry conditions have also been reported from central-west and southwestern Patagonia, concurrent with peak fire activity in South America south of 30°S (Power et al., 2008; Whitlock et al., 2007). Similar findings from other mid-latitude landmasses indicate diminished SWW influence throughout the southern mid-latitudes, suggesting a zonally symmetric decline in SWW strength during the early Holocene (between ~11,000 and 8000 cal. yr BP) (Fletcher and Moreno, 2012). The Lago Pichilaguna record shows the appearance and persistence of lowland deciduous forests at 10,000 cal. yr BP, as indicated by the appearance of *Nothofagus obliqua* type pollen. This shift is also evident in the Canal de la Puntilla + Huelmo spliced pollen record (Moreno et al., 2015), as well as the palynology from marine cores ODP1233 and 1234 (Heusser et al., 2006a, 2006b) (Fig. 12). We note that the abundance of *N. obliqua* type is significantly higher in the ODP1234 record, located 550 km north of Lago Pichilaguna and ODP1233, suggesting that the core distribution of lowland deciduous forests must have lain north of the Chilean Lake District.

4.5. Paleoclimate implications II: the last 8000 years

Extreme warm/dry conditions ended at ~7800 cal. yr BP in the majority of palynological records from northwestern Patagonia during a period of rising lake level (Abarzua et al., 2004; Moreno and Videla, 2016; Pesce and Moreno, 2014), declines in the summer-drought tolerant and thermophilous VRF tree *Eucryphia/Caldcluvia* (Fig. 12) and much diminished fire activity (Moreno, 2004; Moreno and Videla, 2016). This interval in Lago Pichilaguna features finely laminated facies with algal blooms which correspond with a period of relatively increasing oxic conditions in the lake (lower Fe/Mn) at 9200–9100, 8000–7730, 6800–6750, 6600–6200, and 6100-5700 cal. yr BP (Fig. 6), indicative of better mixing conditions likely associated with stronger wind activity and/or lower lake levels. Unlike coastal sites in the region (Lagos Condorito and El Salto) (Moreno, 2004; Moreno and Videla, 2016), Lago Pichilaguna features a major increase in *Eucryphia/Caldcluvia* and enhanced fire activity between 6400 and 2600 cal. yr BP (Figs. 7, 8 and 10). This difference between coastal sites and a site located in the Longitudinal Valley was first noted by Jara and Moreno (2014) in the Lago Pichilafquén record, a small closed-basin site located ~75 km northeast of Lago Pichilaguna in the northern portion of the Longitudinal Valley of the Chilean Lake District. The divergence was attributed to heterogeneities at the landscape level caused by disturbance in the vicinity of Lago Pichilaguna, considering that *Eucryphia/Caldcluvia* and macroscopic charcoal showed consistent statistically significant increases following the deposition of numerous tephra since 8000 cal. yr BP (Jara and Moreno, 2014). When comparing the Lago Pichilaguna and Lago Pichilafquén records we note striking similarities in the timing, rate and direction of *Eucryphia/Caldcluvia* over the last 10,000 years despite a stark contrast in the number and thickness of tephra layers over the last ~11,000 years, i.e. 3 vs 22 fallout tephra levels (pyroclastic material delivered to the site primarily through aerial deposition) in Lago Pichilaguna and Lago Pichilafquén respectively. Aspects common to both records include their location in the lowlands of the Longitudinal Valley north of 41°30′S and intense fire activity over the last 10,000 years. We posit that the rainshadow effect of the Coastal Range on sectors of the Longitudinal Valley where the Lago Pichilaguna and Lago Pichilafquén sites are located, has generated conditions favourable for fire occurrence over the last 10,000 years, affecting the composition and dynamics of terrestrial ecosystems (Fig. 1). Coastal sites in the southern lowlands of the Longitudinal Valley (Lagos Condorito and El Salto) are unaffected by this rainshadow because the Coastal Range is locally interrupted along a ~100 km gap (40°20′S-42°06′S) that extends just south of the latitude of Lago Pichilaguna to northern Isla Grande de Chiloé. This difference could account for the vegetation and fire-history contrasts between lowland sectors located only 40 km apart in the mainland (Fig. 13), i.e. a major increase in *Eucryphia/Caldcluvia* in Lagos Pichilaguna and Pichilafquén starting at ~6400 cal. yr BP whereas Lagos Condorito, El Salto, and Lepué (Pesce and Moreno, 2014) (Fig. 1) show a declining trend since ~8000 cal. yr BP. If this explanation is correct, why did the vegetation and fire-regime divergence start at ~6400 cal. yr BP, and not earlier? Recently, Moreno & Videla (2016) detected a mid-Holocene onset of centennial-scale variability in a pollen and charcoal record from Lago El Salto, Their record shows that centennial-scale variability commenced at 5300 cal. yr BP and featured increases in *Eucryphia/Caldcluvia* and local fires during warm/dry episodes, which alternated with cold/wet intervals with higher abundance of hygrophilous conifers (*Saxegothaea conspicua, Podocarpus nubigena*) and muted fire activity (Moreno and Videla, 2016). We posit that the direct influence of centennial-scale warm/dry anomalies on the vegetation could have been exacerbated in sectors subject to the rainshadow effect of the Coastal Range, promoting desiccation of fuels and enhanced fire activity which, in turn, may have acted as a catalyst of vegetation change and proliferation of shade-intolerant opportunistic tree species. Our results from L: Pichilaguna, along with the previously published L. Pichilafquén results, suggest that centennial-scale climate variability may have started as early as 6400 cal. yr BP in northwestern Patagonia. The onset of centennial-scale hydroclimate variability at 5800 cal. yr BP in the southwestern Patagonian record from L. Cipreses (51°S) (Moreno et al., 2018), is fully consistent with our findings for the mid-Holocene commencement of high-frequency variability in SWW influence along the core and western flank of the Patagonian Andes, following the warm-dry relatively stable early Holocene.

5. Summary/conclusions

The Lago Pichilaguna record allows examination of past vegetation, fire-regime and climatic changes from centennial to multi-millennial timescales along a time continuum from the LGM to the present. Within the last ~25,000 years we conclude the following:

1. Populations of *Nothofagus* trees were ubiquitous in the lowlands of northwestern Patagonia between ~25,000 and 17,800 cal. yr BP and were interspersed in a matrix of herbs and shrubs commonly found above the modern Andean treeline, suggesting a parkland with varying degrees of openness during the LGM. From palynological and sedimentological evidence we interpret cold and hyperhumid conditions during the LGM (~25,000–17,800 cal. yr BP), with moderate warming during the Varas interstade (22,000–19,200 cal. yr BP) followed by cooling and a precipitation increase during the final LGM stade (19,200–17,800 cal. yr BP). From these results we interpret that the SWW influence at 41°S was stronger than today, aspect we interpret as a northward shift of the SWW during the LGM with millennial-scale structure. Maximum SWW influence at 41°S is evident between 19,200 and 17,800 cal. yr BP. There is little evidence of fire activity during the LGM.
2. Relatively thermophilous trees, vines and epiphytes characteristic of the North Patagonian rainforest increased and diversified between 17,800 and 14,800 cal. yr BP, coeval with decreases in cold-tolerant herbs, and a transition to a more productive lake system. We interpret these rapid changes in the lake and the watershed as the onset of T1 with a warm pulse at 17,800 cal. yr BP and a decline in precipitation at 17,800 cal. yr BP related to a southward shift of the SWW. These signals were synchronous

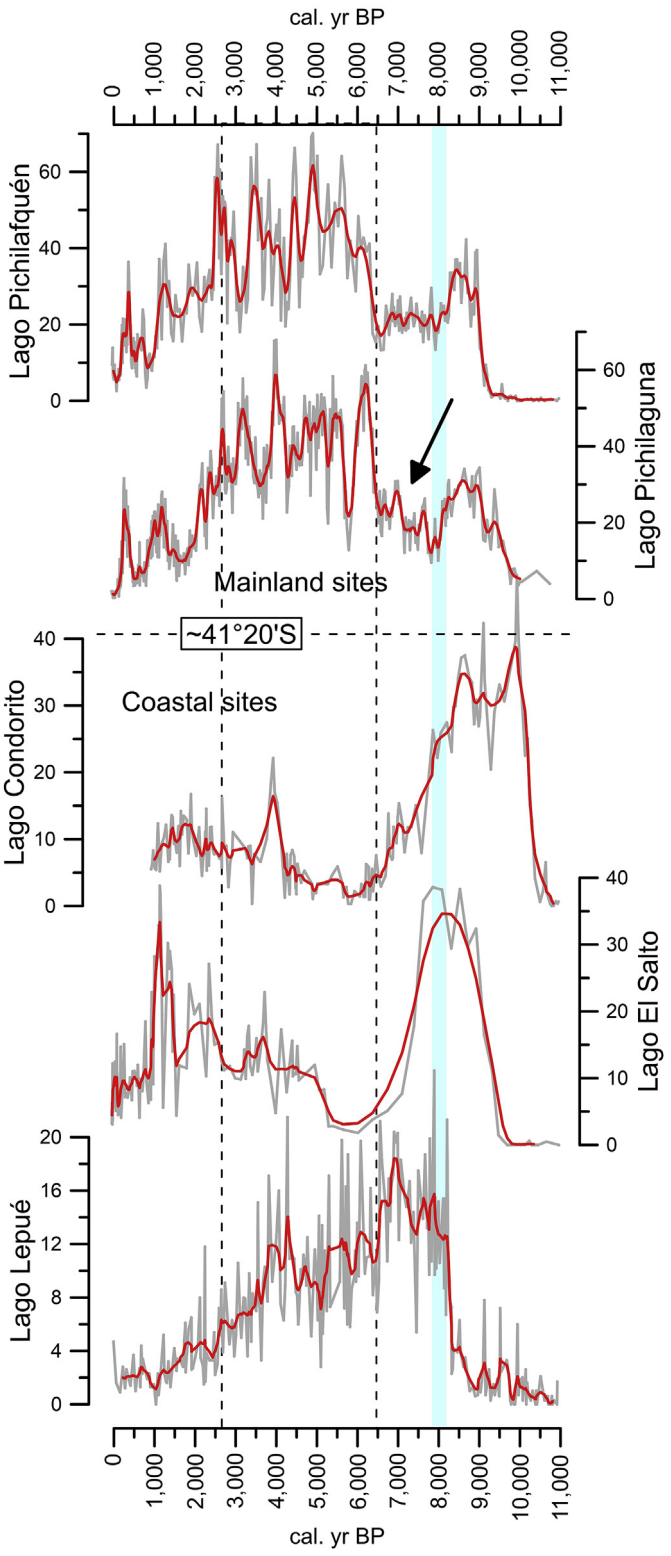

Fig. 13. Comparison of variations in the Eucryphia/Caldcluvia palynomorph from the Lago Pichilaguna record with several sites from northwestern Patagonia over the last 11,000 years. The dashed vertical lines constrain the timing of major divergences in the stratigraphy of Eucryphia/Caldcluvia among coastal and inland sites. The light blue vertical ribbon and the downward pointing arrow highlight the onset of a declining trend in Eucryphia/Caldcluvia abundance common to all records. (For interpretation of the references to color in this figure legend, the reader is referred to the Web version of this article.)

with collapse of the Patagonian ice sheet along a broad latitudinal band (40°-54°S). Fires are practically absent over this interval despite the rapid increase in biomass associated with the spread and densification of forest communities.

3. Closed-canopy North Patagonian rainforests dominated the landscape near Lago Pichilaguna between 16,600 and 15,000 cal. yr BP coeval with high lake productivity under peak interstadial warmth. Fire activity was extremely low despite the abundance of woody biomass susceptible for burning, and the fact that climate had achieved the warmest conditions during the LGM and following T1.
4. Hygrophilous cold-tolerant conifers increased between 14,800 and 11,700 cal. yr BP indicating a shift toward lower temperatures. The interval between 14,800 and 12,700 cal. yr BP (Antarctic Cold Reversal [ACR] chronozone) featured cold and wet conditions, followed by a decline in precipitation between 12,700 and 11,700 cal. yr BP (Younger Dryas [YD] chronozone). We infer an increase in SWW influence at 41°S during the ACR and a decline during the YD, possibly related to a southward shift of the SWW during the latter. Frequent low-magnitude fires during YD time drove a rapid increase in the plants favoured by disturbance (the tree *Weinmannia trichosperma* and Poaceae [possibly the bamboo *Chusquea*]).
5. The thermophilous drought-tolerant tree *Eucryphia/Caldcluvia* characteristic of the Valdivian rainforest, established during the early Holocene (11,700–7700 cal. yr BP), concurrent with lake level lowering, the highest lake organic productivity and maximum frequency in local high-magnitude fire episodes. We interpret these signals as maximum temperature and minimum SWW influence at 41°S.
6. Lowland deciduous forests established at ~10,000 cal. yr BP in sectors of the Longitudinal Valley just north of Lago Pichilaguna. We infer that the southern limit of this deciduous community has remained stable during the Holocene, considering the persistent and low abundance of *Nothofagus obliqua* type in the Lago Pichilaguna record.
7. A major transition at ~7700 cal. yr BP is evident in multiple palynological sites in northwestern Patagonia, with the onset of a multi-millennial trend toward cooler and wetter conditions. After this transition we note divergences in the behaviour of vegetation and fire regimes in mainland and coastal sites located north and south of ~41°20′S.
8. We detect centennial-scale variability superimposed upon a precipitation rise between 7700 and 3200 cal yr BP. We infer that the SWW experienced large-magnitude changes in their latitudinal position from 6400 cal. yr BP onward and led to intense disturbance by fires that shaped the composition of the native vegetation. A shift from laminated to massive sedimentary facies at about 5200 cal. yr BP suggest a lake level increase and lower dominance of diatoms as main producers. A decline in SWW influence started at ~3200 cal. yr BP with centennial-scale changes that persist until the present.
9. Rapid deforestation and spread of invasive exotic species aided by fires set by Chilean-European at ~350 cal. yr BP. The scale and rapidity of this disturbance event exceeded the resilience of temperate rainforests and led to deforestation, increased soil erosion and establishment of pasturelands and agricultural fields. This event constitutes the fastest/largest-magnitude vegetation change of the entire ~25,000-year long record.

Acknowledgements

Funded by Fondecyt 1151469 and 1160488, Núcleo Milenio Paleoclima and NC120066 of Iniciativa Científica Milenio del Ministerio de Economía, Fomento y Turismo (Chile), and the

Universidad de Chile–CSIC collaborative program (2011–2012). We thank Pablo Corella, Michael Fletcher, Mario Morellón and Oscar Pesce for their help during field work, Loreto Hernández for laboratory assistance, and T. Guilderson, S. Collado and R. De Pol for analyzing the radiocarbon samples.

Appendix A. Supplementary data

Supplementary data related to this article can be found at https://doi.org/10.1016/j.quascirev.2018.08.013.

References

Abarzua, A.M., Villagran, C., Moreno, P.I., 2004. Deglacial and postglacial climate history in east-central Isla Grande de Chiloe, southern Chile (43 degrees S). Quat. Res. 62, 49–59.
Alloway, B.V., Almond, P.C., Moreno, P.I., Sagredo, E., Kaplan, M.R., Kubik, P.W., Tonkin, P.J., 2018. Mid-latitude trans-Pacific reconstructions and comparisons of coupled glacial/interglacial climate cycles based on soil stratigraphy of cover-beds. Quat. Sci. Rev. 189, 57–75.
Alloway, B.V., Moreno, P.I., Pearce, N.J.G., De Pol-Holz, R., Henriquez, W.I., Pesce, O.H., Sagredo, E., Villarosa, G., Outes, V., 2017. Stratigraphy, age and correlation of Lepue Tephra: a widespread c. 11 000 cal a BP marker horizon sourced from the Chaiten Sector of southern Chile. J. Quat. Sci. 32, 795–829.
Andersen, B., Denton, G.H., Lowell, T.V., 1999. Glacial geomorphologic maps of llanquihue drift in the area of the southern lake district, Chile. Geogr. Ann. Phys. Geogr. 81, 155–166.
Bao, R., Hernández, A., Sáez, A., Giralt, S., Prego, R., Pueyo, J.J., Moreno, A., Valero-Garcés, B.L., 2015. Climatic and lacustrine morphometric controls of diatom paleoproductivity in a tropical Andean lake. Quat. Sci. Rev. 129, 96–110.
Blaauw, M., Christen, J.A., 2011. Flexible paleoclimate age-depth models using an autoregressive gamma process. Bayesian Analysis 6, 457–474.
Denton, G.H., Anderson, R.F., Toggweiler, J.R., Edwards, R.L., Schaefer, J.M., Putnam, A.E., 2010. The last glacial termination. Science 328, 1652–1656.
Denton, G.H., Broecker, W.S., Alley, R.B., 2006. The mystery interval 17.5 to 14.5 kyrs ago. PAGES News 14, 14–16.
Denton, G.H., Heusser, C.J., Lowell, T.V., Moreno, P.I., Andersen, B.G., Heusser, L.E., Schluchter, C., Marchant, D.R., 1999a. Interhemispheric linkage of paleoclimate during the last glaciation. Geogr. Ann. Phys. Geogr. 81A, 107–153.
Denton, G.H., Lowell, T.V., Heusser, C.J., Schluchter, C., Andersen, B.G., Heusser, L.E., Moreno, P.I., Marchant, D.R., 1999b. Geomorphology, stratigraphy, and radiocarbon chronology of Llanquihue drift in the area of the southern Lake District, Seno Reloncavi, and Isla Grande de Chiloe, Chile. Geogr. Ann. Phys. Geogr. 81A, 167–229.
Donoso Zegers, C., 2006. Las especies arbóreas de los bosques templados de Chile y Argentina : autoecología. Cuneo, Valdivia.
Faegri, K., Iversen, J., 1989. Textbook of Pollen Analysis. John Wiley & Sons.
Fletcher, M.S., Moreno, P.I., 2012. Have the Southern Westerlies changed in a zonally symmetric manner over the last 14,000 years? A hemisphere-wide take on a controversial problem. Quat. Int. 253, 32–46.
Fogt, R.L., Bromwich, D.H., Hines, K.M., 2011. Understanding the SAM influence on the south pacific ENSO teleconnection. Clim. Dynam. 36, 1555–1576.
Frugone-Álvarez, M., Latorre, C., Giralt, S., Polanco-Martínez, J., Bernárdez, P., Oliva-Urcia, B., Maldonado, A., Carrevedo, M.L., Moreno, A., Delgado Huertas, A., Prego, R., Barreiro-Lostres, F., Valero-Garcés, B., 2017. A 7000-year high-resolution lake sediment record from coastal central Chile (Lago Vichuquén, 34°S): implications for past sea level and environmental variability. J. Quat. Sci. 12, 830–844.
Garreaud, R.D., 2007. Precipitation and circulation covariability in the extratropics. J. Clim. 20, 4789–4797.
Garreaud, R.D., Vuille, M., Compagnucci, R., Marengo, J., 2009. Present-day south american climate. Palaeogeogr. Palaeoclimatol. Palaeoecol. 281, 180–195.
Gonzalez, M.E., Veblen, T.T., Donoso, C., Valeria, L., 2002. Tree regeneration responses in a lowland Nothofagus-dominated forest after bamboo dieback in South-Central Chile. Plant Ecol. 161, 59–73.
Grimm, E.C., Jacobson, G.L., 1992. Fossil-pollen evidence for abrupt climatic changes during the past 18,000 years in eastern North America. Clim. Dynam. 6, 179–184.
Heusser, C.J., 1966. Late-Pleistocene pollen diagrams from the Province of Llanquihue, southern Chile. Proc. Am. Phil. Soc. 110, 269–305.
Heusser, C.J., 1971. Pollen and Spores from Chile. University of Arizona Press, Tucson.
Heusser, C.J., 2003. Ice Age Southern Andes: a Chronicle of Palaeoecological Events. Elsevier Science.
Heusser, C.J., Heusser, L.E., Lowell, T.V., 1999. Paleoecology of the southern Chilean Lake District- Isla Grande de Chiloé during middle-Late Llanquihue glaciation and deglaciation. Geogr. Ann. Phys. Geogr. 81 A, 231–284.
Heusser, L., Heusser, C., Mix, A., McManus, J., 2006a. Chilean and Southeast Pacific paleoclimate variations during the last glacial cycle: directly correlated pollen and δ18O records from ODP Site 1234. Quat. Sci. Rev. 25, 3404–3415.
Heusser, L., Heusser, C., Pisias, N., 2006b. Vegetation and climate dynamics of southern Chile during the past 50,000 years: results of ODP Site 1233 pollen analysis. Quat. Sci. Rev. 25, 474–485.
Hickey, R.J., Macluf, C., Taylor, W.C., 2003. A Re-Evaluation of Isoetes savatieri Franchet in Argentina and Chile. Am. Fern J. 93, 126–136.
Higuera, P.E., Brubaker, L.B., Anderson, P.M., Hu, F.S., Brown, T.A., 2009. Vegetation mediated the impacts of postglacial climate change on fire regimes in the south-central Brooks Range, Alaska. Ecol. Monogr. 79, 201–219.
Holz, A., Kitzberger, T., Paritsis, J., Veblen, T.T., 2012. Ecological and climatic controls of modern wildfire activity patterns across southwestern South America. Ecosphere 3, 1–25.
Iglesias, V., Quintana, F., Nanavati, W., Whitlock, C., 2016. Interpreting modern and fossil pollen data along a steep environmental gradient in northern Patagonia. Holocene 27, 1008–1018.
Jara, I.A., Moreno, P.I., 2012. Temperate rainforest response to climate change and disturbance agents in northwestern Patagonia (41 degrees S) over the last 2600 years. Quat. Res. 77, 235–244.
Jara, I.A., Moreno, P.I., 2014. Climatic and disturbance influences on the temperate rainforests of northwestern Patagonia (40 °S) since ~14,500 cal yr BP. Quat. Sci. Rev. 90, 217–228.
Lambert, F., Bigler, M., Steffensen, J.P., Hutterli, M., Fischer, H., 2012. Centennial mineral dust variability in high-resolution ice core data from Dome C, Antarctica. Clim. Past 8, 609–623.
Lara, A., Villalba, R., Wolodarsky-Franke, A., Aravena, J.C., Luckman, B.H., Cuq, E., 2005. Spatial and temporal variation in Nothofagus pumilio growth at tree line along its latitudinal range (35 degrees 40 '-55 degrees S) in the Chilean Andes. J. Biogeogr. 32, 879–893.
McCormac, F.G., Hogg, A.G., Blackwell, P.G., Buck, C.E., Higham, T.F.G., Reimer, P.J., 2004. SHCal04 Southern Hemisphere calibration, 0-11.0 cal kyr BP. Radiocarbon 46, 1087–1092.
Mercer, J.H., 1972. Chilean Glacial Chronology 20,000 to 11,000 Carbon-14 years ago: some global comparisons. Science 172, 1118–1120.
Monnin, E., Indermuhle, A., Dallenbach, A., Fluckiger, J., Stauffer, B., Stocker, T.F., Raynaud, D., Barnola, J.M., 2001. Atmospheric CO2 concentrations over the last glacial termination. Science 291, 112–114.
Moreno, A., Giralt, S., Valero-Garcés, B., Sáez, A., Bao, R., Prego, R., Pueyo, J.J., González-Sampériz, P., Taberner, C., 2007. A 14kyr record of the tropical andes: the lago Chungará sequence (18 S, northern Chilean altiplano). Quat. Int. 16, 4–21.
Moreno, P.I., 2004. Millennial-scale climate variability in northwest Patagonia over the last 15000 yr. J. Quat. Sci. 19, 35–47.
Moreno, P.I., Denton, G.H., Moreno, H., Lowell, T.V., Putnam, A.E., Kaplan, M.R., 2015. Radiocarbon chronology of the last glacial maximum and its termination in northwestern Patagonia. Quat. Sci. Rev. 122, 233–249.
Moreno, P.I., Jacobson, G.L., Andersen, B.G., Lowell, T.V., Denton, G.H., 1999. Abrupt vegetation and climate changes during the last glacial maximum and the last Termination in the Chilean Lake District: a case study from Canal de la Puntilla (41°S). Geogr. Ann. Phys. Geogr. 81 A, 285–311.
Moreno, P.I., Leon, A.L., 2003. Abrupt vegetation changes during the last glacial to Holocene transition in mid-latitude South America. J. Quat. Sci. 18, 787–800.
Moreno, P.I., Videla, J., 2016. Centennial and millennial-scale hydroclimate changes in northwestern Patagonia since 16,000 yr BP. Quat. Sci. Rev. 149, 326–337.
Moreno, P.I., Vilanova, I., Villa-Martínez, R., Dunbar, R.B., Mucciarone, D.A., Kaplan, M.R., Garreaud, R.D., Rojas, M., Moy, C.M., Pol-Holz, R.D., Lambert, F., 2018. Onset and evolution of southern annular mode-like changes at centennial timescale. Sci. Rep. 8, 3458.
Naeher, S., Gilli, A., North, R.P., Hamann, Y., Schubert, C.J., 2013. Tracing bottom water oxygenation with sedimentary Mn/Fe ratios in Lake Zurich, Switzerland. Chem. Geol. 352, 125–133.
Oberdorfer, E., 1960. Pflanzensoziologische Studien in Chile. Cramer, Weinheim, pp. 1–208.
Pesce, O.H., Moreno, P.I., 2014. Vegetation, fire and climate change in central-east Isla Grande de Chiloé (43°S) since the Last Glacial Maximum, northwestern Patagonia. Quat. Sci. Rev. 90, 143–157.
Power, M.J., Marlon, J., Ortiz, N., Bartlein, P.J., Harrison, S.P., Mayle, F.E., Ballouche, A., Bradshaw, R.H.W., Carcaillet, C., Cordova, C., Mooney, S., Moreno, P.I., Prentice, I.C., Thonicke, K., Tinner, W., Whitlock, C., Zhang, Y., Zhao, Y., Ali, A.A., Anderson, R.S., Beer, R., Behling, H., Briles, C., Brown, K.J., Brunelle, A., Bush, M., Camill, P., Chu, G.Q., Clark, J., Colombaroli, D., Connor, S., Daniau, A.L., Daniels, M., Dodson, J., Doughty, E., Edwards, M.E., Finsinger, W., Foster, D., Frechette, J., Gaillard, M.J., Gavin, D.G., Gobet, E., Haberle, S., Hallett, D.J., Higuera, P., Hope, G., Horn, S., Inoue, J., Kaltenrieder, P., Kennedy, L., Kong, Z.C., Larsen, C., Long, C.J., Lynch, J., Lynch, E.A., McGlone, M., Meeks, S., Mensing, S., Meyer, G., Minckley, T., Mohr, J., Nelson, D.M., New, J., Newnham, R., Noti, R., Oswald, W., Pierce, J., Richard, P.J.H., Rowe, C., Goni, M.F.S., Shuman, B.N., Takahara, H., Toney, J., Turney, C., Urrego-Sanchez, D.H., Umbanhowar, C., Vandergoes, M., Vanniere, B., Vescovi, E., Walsh, M., Wang, X., Williams, N., Wilmshurst, J., Zhang, J.H., 2008. Changes in fire regimes since the Last Glacial Maximum: an assessment based on a global synthesis and analysis of charcoal data. Clim. Dynam. 30, 887–907.
Sagredo, E.A., Kaplan, M.R., Araya, P.S., Lowell, T.V., Aravena, J.C., Moreno, P.I., Kelly, M.A., Schaefer, J.M., 2018. Trans-pacific glacial response to the Antarctic Cold Reversal in the southern mid-latitudes. Quat. Sci. Rev. 188, 160–166.
Schmithüsen, J., 1956. Die raumliche Ordnung der chilenischen Vegetation. Bonn. Geogr. Abh. 17, 1–86.
Schnurrenberger, D., Russell, J., Kelts, K., 2003. Classification of lacustrine sediments based on sedimentary components. J. Paleolimnol. 29, 141–154.

Stenni, B., Masson-Delmotte, V., Selmo, E., Oerter, H., Meyer, H., Rothlisberger, R., Jouzel, J., Cattani, O., Falourd, S., Fischer, H., Hoffmann, G., Iacumin, P., Johnsen, S.J., Minster, B., Udisti, R., 2010. The deuterium excess records of EPICA Dome C and Dronning Maud Land ice cores (East Antarctica). Quat. Sci. Rev. 29, 146–159.

Stuiver, M., Pearson, G.W., 1993. High-precision bidecadal calibration of the radiocarbon time scale, ad 1950-500 Bc and 2500-6000 bc. Radiocarbon 35, 1–23.

Thompson, D.W.J., Solomon, S., Kushner, P.J., England, M.H., Grise, K.M., Karoly, D.J., 2011. Signatures of the Antarctic ozone hole in Southern Hemisphere surface climate change. Nat. Geosci. 4, 741–749.

Toggweiler, J.R., 2009. Shifting westerlies. Science 323, 1434–1435.

Toggweiler, J.R., Russell, J.L., Carson, S.R., 2006. Midlatitude westerlies, atmospheric CO2, and climate change during the ice ages. Paleoceanography 21. https://doi.org/10.1029/2005PA001154.

Villagrán, C., 1980. Vegetatiosgeschichtliche und pflanzensoziologische Untersuchungen im Vicente Perez Rosales Nationalpark (Chile). Diss. Bot. 54, 1–165.

Villagrán, C., 1985. Análisis palinológico de los cambios vegetacionales durante el Tardiglacial y Postglacial en Chiloé, Chile. Rev. Chil. Hist. Nat. 58, 57–69.

WAIS Divide Project Members, 2013. Onset of deglacial warming in West Antarctica driven by local orbital forcing. Nature 500, 440–444.

Whitlock, C., Anderson, R.S., 2003. Fire history reconstructions based on sediment records from lakes and wetlands. In: Veblen, T.T., Baker, W.L., Montenegro, G., Swetnam, T.W. (Eds.), Fire and Climatic Change in Temperate Ecosystems of the Western Americas. Springer, New York, pp. 265–295.

Whitlock, C., Moreno, P.I., Bartlein, P., 2007. Climatic controls of Holocene fire patterns in southern South America. Quat. Res. 68, 28–36.